

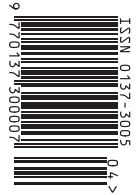


h=663-10-157
i=314592

NR 4 (611) 2025
p-ISSN 0137-3005 | NR-NB 35 550 X
MONTHLY
www.dedami.edu.pl








MATHEMATICS - PHYSICS - ASTRONOMY - INFORMATICS

Can you see
a graph here?
p. 13





CONTENTS OF ISSUE 4 (611) 2025

Mathematical Boundaries? Not Here!	str. 1
Benford's Law	
<i>Owen Barron</i>	str. 2
Hilbert's Irreducibility Theorem	
<i>Navid Safaei, Radosław Żak</i>	str. 4
Can the policemen catch the thief?	
<i>Alexandru Benescu</i>	str. 6
Beyond Classical Limits: The Power and Potential of Quantum Computing	
<i>Pranav Challa</i>	str. 8
 Problems	str. 9
A few different proofs of the Fermat theorem on sum of two squares	
<i>Maryna Spektrova</i>	str. 10
Can you see a graph here?	
<i>Sylwia Sapkowska</i>	str. 13
 Aktualności	
Soft-boiled, hard-boiled... and just right	str. 17
 First and Foremost: Laughter	
<i>Marta Fikus-Kryńska</i>	str. 18
 Łat Otwarty: $14 = 2 \cdot 7$	
<i>Bartłomiej Pawlik</i>	str. 19
Club 44	str. 20
 The Sky in April	str. 22
 Straight from Heaven: Again, That Mass Gap	str. 23
 Rotations by Certain Special Angles	
<i>Bartłomiej Bzdega</i>	str. 25

Delta Monthly Magazine – Mathematics, Physics, Astronomy, Informatics is published by the University of Warsaw in collaboration with scientific societies: the Polish Mathematical Society, Polish Physical Society, Polish Astronomical Society, and Polish Information Processing Society.

Editorial Committee: dr Waldemar Berej;
dr Piotr Chrzastowski-Wachtel, prof. UW;
dr Krzysztof Ciesielski, prof. UJ – President;
dr hab. Wojciech Czerwiński, prof. UW;
prof. dr hab. Sławomir Dinew; dr Tomasz Greczyło, prof. UW;
dr Adam Gregosiewicz; prof. dr hab. Agnieszka Janiuk;
dr Joanna Jaszuńska; dr hab. Artur Jeż, prof. UW;
prof. dr hab. Bartosz Klin; dr Piotr Kołaczek-Szymański;
prof. dr hab. Andrzej Majhofer – vice-President;
dr Adam Michalec; prof. dr hab. Damian Niwiński;
dr hab. Krzysztof Pawłowski, prof. PAN; dr Milena Ratajczak;
dr hab. Radosław Smolec, prof. PAN;
prof. dr hab. Paweł Strzelecki; prof. dr hab. Andrzej Wysłomlek.

Editorial Board: Michał Bejger, Paweł Bieliński,
Szymon Charzyński – Editor-in-Chief, Agnieszka Chudek,
Anna Durkalec, Jan Horubała, Michał Miśkiewicz,
Wojciech Przybyszewski, Łukasz Rajkowski – Deputy
Editor-in-Chief, Anna Rudnik, Marzanna Wawro – secretary of
the Editorial Board.

Correspondence address:
Delta's editorial office, ul. Banacha 2, pokój 4020, 02-097
Warszawa

e-mail: delta@mimuw.edu.pl tel. 22-55-44-402.

Covers and graphics:

Anna Ludwicka Graphic Design & Serigrafia.

Typeset using L^AT_EX by the Editors.

Printed at Arkuszowa Drukarnia Offsetowa Sp. z o.o.

www.ado.com.pl

Subscription:

Garmond Press: www.garmondpress.pl

Kolporter: www.kolporter.com.pl (institutions only)

On the Empik website, *Delta* can be ordered every month:

www.empik.com/delta,p1235643855,prasa-p

Back Issues (from 1987 onwards) can be purchased in person
at the Editorial Office or ordered via email.

Price per copy: for the last 12 months, 6 PLN; for earlier issues,
3 PLN.



Website (including archived
articles, links, etc.):

deltami.edu.pl

You can also find us on

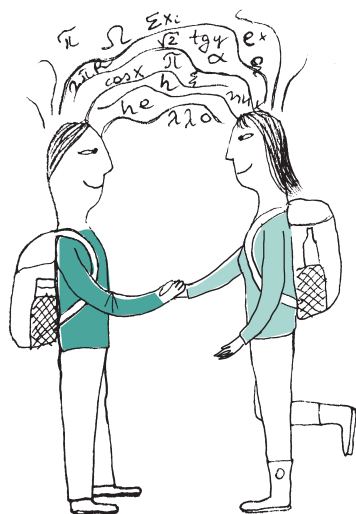
facebook.com/Delta.czasopismo

Publisher: University of Warsaw



-
- Visegrad Fund
-
-

The project is co-financed by the Governments of Czechia, Hungary, Poland and Slovakia through Visegrad Grants from International Visegrad Fund. The mission of the fund is to advance ideas for sustainable regional cooperation in Central Europe.



Mathematical Boundaries? Not Here!

Mathematics knows no limits – neither geographical nor intellectual. A testament to this is Maths Beyond Limits (MBL) – an international camp for high school students passionate about maths. It is a place where young enthusiasts from all over the world come together to explore fascinating, non-school-related areas of this field, develop their analytical and creative skills, and, most importantly, share their passion. MBL creates an open and supportive community where maths is not only an intellectual challenge but also an inspiration to discover new paths in science and in life.

Mathematical Challenges and Beyond

MBL 2024, the ninth edition of this extraordinary event, took place in the picturesque Rycerka Dolna from September 8 to 21. It was attended by 60 participants and 24 tutors from 29 countries, ranging from Europe to Asia and the Americas. Each day of the camp was filled with intense mental work: in addition to three 80-minute blocks of mathematical classes led by experienced tutors, participants also had an hour of TAU (Time Academic Unscheduled) – a time dedicated to independent problem-solving and consultations with tutors. The participants also had the opportunity to learn from each other – some of them presented their favorite topics in half-hour Camper Talks. It is from these lectures and presentations that the articles in this issue originate. The authors are the camp's tutors and participants, who shared their knowledge on fascinating mathematical topics discussed during MBL.

Not Just Mathematics

However, MBL is more than just mathematical challenges. After intense mathematical work, there were Evening Activities – full of fun, challenges, and inspiration, often organized by the participants themselves – ranging from art workshops to philosophical discussions. Sports were also included – from running and exercise to volleyball, football, and frisbee matches – as well as the exciting Puzzle Hunt, a team-based marathon of logical puzzles.

Join the MBL Community!

If you're in high school, feel that maths is your passion, and want to experience learning in a completely new dimension, don't miss the chance to participate in the next edition! If you have already graduated, it is not too late – we are also looking for tutors! Recruitment starts on April 1. More information can be found at mathsbeyondlimits.eu and on our social media.

Cross the boundaries of mathematics – and your own!

MBL organisers

MBL 2024 participants



Benford's Law

Owen BARRON*

* Coláiste an Spioraid Naoimh, University
College Cork Maths Enrichment
Program

I encountered Benford's Law for the first time at a young age while reading through a book on mathematical curiosities. The simplicity and generality of the law made it fascinating to me – especially since it appeared completely impossible at first sight.

Benford's Law is an interesting and at first counter-intuitive statistical phenomenon that occurs in almost all natural data sets that span multiple orders of magnitude. It states that the first digit of items in these sets is much more likely to be small (e.g. 1 or 2) than big (e.g. 8 or 9). The expected distribution is staggeringly weighted towards these small digits. According to the law, 1 occurs as the first digit of about 30% of entries in data sets, whereas 9 appears first in only 5%!

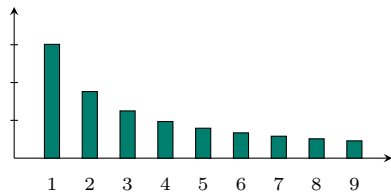


Fig. 1. Frequencies defined by the Benford's Law

Precisely, Benford's Law states that the frequency with which a digit d occurs in a base-10 data set spanning some orders of magnitude of powers of 10 is roughly equal to $\log_{10}(d+1) - \log_{10}(d)$ (Fig. 1). The spanning some orders of magnitude condition is deceptively important – data sets not following this condition rarely follow the law. As an example, the number of pages in books do not for the clear reason that most page counts are somewhere between 200 and 600.

It's difficult to overestimate how broadly this law applies: some data sets that follow it in the real world are the heights of the hundred tallest buildings or the lengths of rivers. Examples even extend to the purely mathematical, such as the Fibonacci series, the series of powers of 2, and even the series obtained from alternating between multiplication by 2 and 3! After hearing about the law for the first time, I was slightly bemused – how could something so blatantly asymmetric hold true in such a generalised sense? This article will aim to provide an intuitive if not formal explanation for why the law holds, as well as some history behind it and surprising places it can be applied in real life.

The law was first discovered in 1881 by Simon Newcomb, a Canadian-American astronomer. He observed that the earlier pages of books of logarithms, used for calculations were much more worn out than those later on. He conjectured that this was due to the data sets scientists were performing calculations on tending towards having numbers with lower starting digits. Newcomb published a brief note on the phenomenon including the theoretical values of probabilities and a short, informal argument explaining why it was true in the American Journal of Mathematics, but it gained minimal traction.

More than fifty years later, in 1938, the law was rediscovered independently by its namesake – Frank Benford. Benford was working in research physics when he discovered the pattern in the same manner that Newcomb had. However, he took his investigation of the law a level deeper and gathered sets of data with 20,000 total items as examples. He used these as evidence in the paper he published in the Proceedings of the American Philosophical Society, aptly titled 'The Law of Anomalous Numbers'. Unfortunately this name did not stick, and the law was instead called after Benford, giving us another example of Stigler's Law in the mathematical world.

The reader may be forgiven for some skepticism about all of the above at this point – but what may at first seem like an impossible phenomenon luckily has a simple and intuitive explanation. Say we have a set of numbers spanning multiple orders of magnitude. We would expect the data points to be roughly evenly distributed among these orders – e.g there are roughly the same number of items in the interval $[100, 1000]$ as $[1000, 10000]$. On the logarithmic scale those two intervals have the same length $\log_{10} 10 = 1$. By extrapolation we may expect that for any two segments of equal length on the logarithmic scale the number of items falling in either of them is roughly the same. In other words, we expect the data points to be evenly spread on the logarithmic scale. The set of

Stigler's Law states that discoveries are relatively rarely named after the people who made them. One example of this is Stigler's Law itself.

We refer the reader to the article *Od mnożenia do dodawania* (Δ_{25}^{01}) for further interesting information on the logarithmic scale

numbers whose base 10 representation starts with a digit d is a disjoint union of sequences of length $\log_{10}(d+1) - \log_{10}(d)$, which leads us to the probability given by the Benford's law.

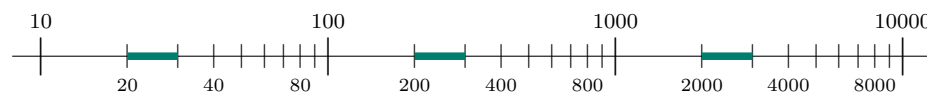


Fig. 2. Coloured segments of length $\log_{10}(3) - \log_{10}(2)$ correspond to having '2' as the first digit

Let us note that the above reasoning does not constitute a full *proof of correctness* of Benford's Law. Theoreticians may argue that a „uniform distribution” does not exist over the entire infinite logarithmic scale, while practitioners may ask why we actually are focusing on a uniform distribution in the logarithmic scale — whether this is a law of nature or if it also follows from mathematical theorems of the kind found in the central limit theorem. For readers who find this explanation unsatisfactory, we recommend Ted Hill's article *A Statistical Derivation of the Significant-Digit Law*, published in *Statistical Science* in 1995.

Unlike many high-level mathematical theorems, there are a surprising number of situations in the real world where direct application of the law becomes extremely useful. The most important of these applications occur in the field of fraud detection, where it is often used as a preliminary test to find faults. Accounting books normally follow Benford's Law, as would be expected from a roughly random distribution over several orders of magnitude. However, when random numbers are generated by computer or by hand in fabricated accounts, one would expect them to instead have evenly distributed digits. After first hearing about Benford's Law, financial investigator Darrell D. Dorrell immediately began applying it to cases he was working on. This led to the successful conviction of Wesley Rhodes, a financial advisor who embezzled millions of dollars in funds from his investors. The law is regularly used as a first indicator or red flag of financial fraud – if the figures in checkbooks do not follow the law, it is likely some kind of anomaly is at play.

One other very interesting use was the uncovering of a hidden bot network on Twitter. Jennifer Golbeck noticed in 2015 that for the majority of users, the number of followers that their followers have adheres to Benford's Law. However, a small percentage of accounts investigated did not adhere to the pattern. These 170 accounts were flagged and investigated further, by examining their followers and post history. Out of all 170 only 2 seemed to belong to legitimate users. The rest of the accounts all had followers among the other accounts, and clearly automated or otherwise suspicious posts.

However, the law has strong failings when it comes to some other attempted uses, especially in election fraud. There is a simple reason for this: electoral districts normally have similar populations. Thus if one candidate expects to receive a certain percentage of votes in each of these districts, their first digit distribution will be confined to a range not necessarily following Benford's Law. Similarly for financial fraud, if a company sells a large number of a product that has a specific price, the digit distribution in accounts will be weighted towards the first digit of this product. In the 2020 US presidential race, conspiracists noticed that Joe Biden's vote counts in some areas did not follow the law. They were quick to raise this issue as an indicator

of a rigged election, but for the reasons above they were proven to be mistaken in doing so.

Somewhat surprisingly, a much weaker version of the law holds for the second digit of numbers in data sets as well – in these cases, the difference in occurrences between 0 and 9 as the second digit is only about 3% – but this is still recognizable in large enough sets. There is in fact a distribution in the general case for the n^{th} digit, although it becomes flatter and flatter as n increases. In the application of Benford's Law to elections, it is this generalisation in combination with the first digit law that allows a decision on whether or not fraud exists to be much more reliable. The second digit of a number will clearly be less affected in general by the similarity of electoral district populations than the first digit.

The n^{th} digit is not the only generalisation of the law. It also holds when the data points are converted into any other base, and even when the data points are converted from one unit into another. In my research on the topic, I discovered other similarly surprising results too – if you are interested, Zipf's Law on the frequency of words in texts is fascinating. I am still surprised every time the law shows up in my day-to-day life – if you start searching for it, you may begin to see examples everywhere you go!

Hilbert's Irreducibility Theorem

Navid SAFAEI*, Radosław ŻAK**

*Head of Mathematical Olympiad department, Salam Schools Complex, Tehran, Iran Institute of Mathematics and Informatics, Bulgarian Academy of Sciences, Sofia
 **PhD student, University of Oxford



Number theory is among fields of mathematics which use methods from other areas the most. One incoming stream of tools comes from mathematical analysis. Over the past years analytical number theory got increasingly popular even in the context of mathematical olympiads; Tomek Kobos's article in Δ_{16}^3 showcases a nice selection of common methods. However, the 'alien' concepts of limits, series, convergence and derivatives might be slightly intimidating for students new to this area. One of advantages of Hilbert's Irreducibility Theorem (HIT for short) is that it packs a lot of insight from analysis and/or algebraic geometry in an understandable, number theoretical form.

Recall that a *polynomial in two variables* $P(x, y)$ is a finite sum of monomials, each of which has a form $a_{ij}x^i y^j$. We will mostly work in the case when numbers a_{ij} are integers; the set of all such polynomials will be denoted by $\mathbb{Z}[x, y]$. Among examples we can list $x^3 - y^2$, $x^2 - 2xy + 2y^2$ or $x^3 - x^2y + y^4 + 1$. Another example is $y^3 - 2y + 1$, although it doesn't contain the variable x , and we might want to be careful about that. We have the corresponding notion of the degree for two-variable polynomials – by definition, the degree of monomial $a_{ij}x^i y^j$ is $i + j$, and the *degree of a polynomial* is the maximum of degrees of its monomials. We can also define the *degree in a particular variable*; the degree of $P(x, y)$ in x is just the usual degree if we forget about the fact that y is a variable. For instance, the polynomial $P(x, y) = x^3 - x^2y^3 + y^4 + 2$ has

$$\deg P(x, y) = 5, \quad \deg_x P(x, y) = 3, \quad \deg_y P(x, y) = 4.$$

Similarly as in one-variable case, we say $P(x, y)$ is *reducible* if it can be written as a product $P_1(x, y)P_2(x, y)$ where P_1, P_2 are non-constant polynomials; otherwise we say it's *irreducible*. A well-known tool called Gauss' Lemma implies that if $P(x, y)$ has integer coefficients and it decomposes as $P_1(x, y) \cdot P_2(x, y)$, where P_1, P_2 have **rational** coefficients, then we can also find such an example of P_1, P_2 with **integer** coefficients.

As with primes and integers, irreducible polynomials can be thought of as building blocks: any polynomial $P(x, y)$ can be written as a product $Q_1(x, y)^{\alpha_1} \cdot \dots \cdot Q_k(x, y)^{\alpha_k}$, for some irreducible polynomials Q_1, \dots, Q_k and some positive integer exponents α_i .

Theorem 1 (Hilbert). Let $P(x, y)$ be an irreducible polynomial with integer coefficients, which is dependent on the variable x (i.e., $\deg_x P(x, y) > 0$). Then we can find infinitely many integers t for which the (one-variable) polynomial $f_t(y) := P(t, y)$ is also irreducible, and moreover $\deg f_t = \deg_y P(t, y)$.

An easy example: $Q(x, y) = y^2 - x$ is irreducible. If we try to put $t = 1$, then the polynomial $Q(1, y) = y^2 - 1$ factors as $(y - 1)(y + 1)$. However it's not hard to see that such factorisation occurs precisely when t is a square – thus, we can choose any t which is not a square, and obtain an irreducible polynomial. We can go even further.

Proposition 2. Suppose $R(x)$ is a polynomial with integer coefficients such that $R(t)$ is a square for any integer t . Then there is a polynomial $Q(x)$ with integer coefficients such that $R(x) = Q(x)^2$.

Proof. Consider the polynomial $P(x, y) = y^2 - R(x)$. Suppose it is irreducible. Then by HIT we can find an integer t such that $P(t, y)$ is irreducible. But we know $R(t) = a^2$ for some a , and so $P(t, y) = y^2 - a^2 = (y - a)(y + a)$ is reducible. This contradiction means that $P(x, y)$ is reducible.

Therefore we can find P_1, P_2 with integer coefficients, non-constant, so that $P(x, y) = P_1(x, y)P_2(x, y)$. If $\deg_y P_1 = 0$ (so P_1 doesn't contain y), then P_1 would depend only on x , and it would have to divide the leading coefficient of y in $P(x, y)$. But this is 1, so this is impossible. Hence the only possible case is that

A curious reader can find the proof of HIT in:

M. Villarino, W. Gasarch, K. Regan, *Hilbert's Proof of His Irreducibility Theorem*, Amer. Math. Monthly (2018), doi.org/10.1080/00029890.2018.1448181, arXiv:1611.06303

both P_1 and P_2 are linear in y (as $\deg_y P(x, y) = 2$). But then by examining leading coefficients again, we get that $P_1(x, y) = y + Q_1(x)$, $P_2(x, y) = y + Q_2(x)$ for some polynomials Q_1, Q_2 (as those leading coefficients multiply to 1, and we can multiply our polynomials by -1 if needed, without loss of generality). Therefore

$$\begin{aligned} y^2 - R(x) &= P(x, y) = P_1(x, y)P_2(x, y) = (y + Q_1(x))(y + Q_2(x)) \\ &= y^2 + y(Q_1(x) + Q_2(x)) + Q_1(x)Q_2(x). \end{aligned}$$

By comparing coefficients, we get $Q_1(x) + Q_2(x) = 0$, and so $R(x) = -Q_1(x)Q_2(x) = Q_1(x)^2$. \square

In fact, we can prove something even stronger. We will have to use the following, innocently-looking fact. However, we remark this is not easy to prove; one of its proofs involves Chebotarev's theorem.

Theorem 3. If $f(x)$ is an irreducible polynomial with integer coefficients with $\deg f \geq 2$, then there are infinitely many primes p which do not divide $f(t)$ for any integer t .

Our final goal is to prove the following:

Theorem 4. Let $P(x, y) \in \mathbb{Z}[x, y]$ be a polynomial with the following property: for any non-constant arithmetic sequence $(a_n)_{n=-\infty}^{\infty}$ of integers, we can find an index $i \in \mathbb{Z}$ and an integer y such that $P(a_i, y) = 0$. Then there is a polynomial $R(x) \in \mathbb{Q}[x]$ such that $P(x, R(x)) = 0$ identically.

This will generalise our previous Proposition 2 in two ways. First, we no longer need every t to satisfy something, but only sufficiently many such t 's to cover all integer arithmetic sequences. Second, we could be using any polynomial in place of y^2 . A problem at the end of this article illustrates this last observation.

Proof of Theorem 4. First observe that our condition on arithmetic sequences actually gives us infinitely many indices i for which $P(a_i, y) = 0$ has a solution in y . Indeed, we know there is at least one such i , but then $a'_j := a_{i+1+2j}$ is also an arithmetic sequence (these are odd terms of (a_n) if i is even, and even terms if i is odd), which is a subset of (a_n) not containing a_i . This way we get another index, and we can continue this process as long as we want.

We can factor $P(x, y)$ as a product $Q_1(x, y) \cdots Q_k(x, y)$, for some irreducible polynomials Q_j (not necessarily distinct). If any Q_j depends only on x , then we can safely ignore this component, as it only gives us finitely many t 's for which $P(t, y) = 0$ has a solution. Similarly if $Q_j(x, y) = 0$ itself has only finitely many solutions in x and y , we can ignore it – indeed, in both cases the polynomial $P' := P/Q_j$ satisfies both the problem's assumptions and its claim if and only if P does.

We can now use HIT to find numbers t_j such that each $Q_j(t_j, y)$ is an irreducible polynomial, with the same degree in y as $Q_j(x, y)$ originally was. If this degree is at least 2 for every j , then we can use Theorem 3 to obtain primes p_j so that $p_j \nmid Q_j(t_j, y)$, for each j ; moreover we can choose these primes to be pairwise distinct.

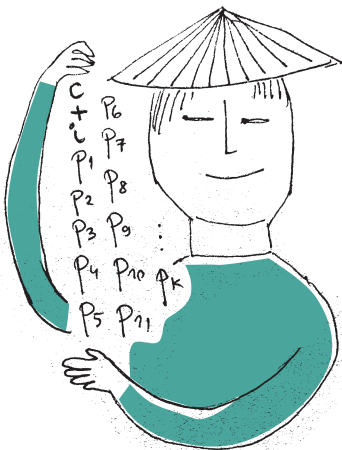
Now let's use Chinese Remainder Theorem to find a solution to the system of congruences $t \equiv t_j \pmod{p_j}$ for $j = 1, \dots, k$. The solution will be of form $t \equiv c \pmod{p_1 p_2 \dots p_k}$ for some c . In other words, the set of solutions forms the arithmetic sequence $a_i = c + ip_1 p_2 \dots p_k$. We know we will find i and y such that $P(a_i, y) = 0$. Therefore, $Q_j(a_i, y) = 0$ for some j . But at the same time

$$Q_j(a_i, y) \equiv Q_j(t_j, y) \not\equiv 0 \pmod{p_j},$$

and so we get a contradiction.

Hence some Q_j is linear in y ; without loss of generality it's Q_1 . We can write $Q_1(x, y) = A(x)y + B(x)$ for A, B polynomials. We already commented why we can assume that each $Q_j(x, y) = 0$ has infinitely many solutions in (x, y) ; therefore $A(x)$ divides $B(x)$ for infinitely many values of x . But this means that

More on Theorem 4 can be found here:
H. Davenport, D. Lewis, A. Schinzel,
Polynomials of certain special types,
Acta Arith. (1964),
<http://eudml.org/doc/207456>



$A(x)$ divides $B(x)$ as a polynomial (for that, consider $\gcd(A(x), B(x))$). Therefore $R(x) = -\frac{B(x)}{A(x)}$ is a polynomial, and hence $P(x, R(x)) = Q_1(x, R(x)) = 0$. \square

A careful reader will notice that Theorem 4 only gives R with rational, and not integer, coefficients. Indeed, if we took $P(x, y) = x^2 + x - 2y$, we would get $R(x) = \frac{x(x+1)}{2}$. We finish by presenting a problem illustrating that in some situations we can actually get $R(x)$ to have integer coefficients.

Problem. Suppose P, Q are two polynomials with integer coefficients, such that for any integer n we can find an integer m so that $P(n) = Q(m)$. Prove that then there is a polynomial $R(x)$ with rational coefficients such that $P(x) = Q(R(x))$. Moreover, if polynomial $Q(\frac{x}{k})$ does not have integer coefficients for any $k \geq 2$, prove that $R(x)$ has integer coefficients.

*Student, Tudor Vianu National College of Computer Science, Romania

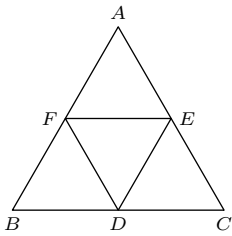


Fig. 1

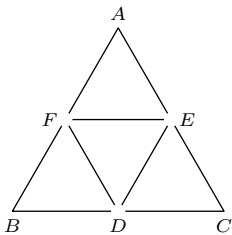


Fig. 2

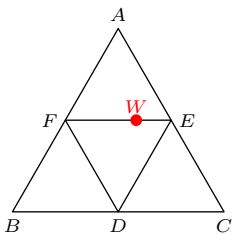


Fig. 3

Can the policemen catch the thief?

Alexandru BENESCU*

In this article, we will address the following problem.

In a village there is a thief and n policemen. The alleys in this village form an equilateral triangle along with its midlines (Fig. 1). The thief's maximum speed is $\kappa > 0$ times greater than the policemen's maximum speed. Given that everyone can see each other and the (continuous) movement is possible only along the alleys, determine whether the policemen can catch the thief from any starting position?

Let us start the solution by analysing some simple cases. Assume that there is only one policeman, i.e. $n = 1$. This situation is trivial. If $\kappa < 1$ (i.e., the thief is slower than the policeman), the policeman has a winning strategy: he can chase the thief regardless of the route the latter takes, eventually catching him. If $\kappa \geq 1$, the thief has a winning strategy by looping in a cycle (such as $A \rightarrow B \rightarrow C \rightarrow A$ in Fig. 1) and adjusting his velocity and direction according to the policeman's movement.

The situation changes drastically (in favour of justice) if there are three (or more) policemen. We prove that in this case they will catch the thief regardless of his speed. One possible strategy for them is to position themselves at points D, E and F , respectively (using the notation of Fig. 1). In this way they partition the whole village into six connected parts (or components), as shown in Fig. 2. One of these parts contains the thief, and this part (like every other one) is closed at both ends by policemen. It is enough for one of them to move towards the other, thus catching the thief.

It remains to consider the case of two policemen, which is more demanding. First, we prove that for $\kappa \leq 3$ the police win. The first policeman is the one to chase the thief (that is why we'll call him *the chaser*). His only task is to prevent the thief from hiding forever in one place. More precisely, he has to make sure that the thief's *last-visited middle node* keeps changing over time (by *middle node* we mean D, E , or F). It is easy to see that only one policeman is enough to ensure this.

The second policeman, whom we'll call *the watcher*, has a more subtle task. Firstly he needs to go to point W that splits the segment EF in a 1:2 ratio (Fig. 3); he does not need to hurry. When he gets there he needs to watch the thief closely (as watchers do). Basically his task is to cut off the thief's escape route whenever possible. For example, if the thief enters the 'upper corner' $E-A-F$ through point E , the watcher must prevent the thief from escaping this corner through point F . It is possible to do so since $\frac{|EA|+|AF|}{|WF|} = 3 \geq \kappa$. There is also one tiny catch – at the same time the thief comes back to the point E , the watcher needs to be back at point W . But this can be ensured

if the watcher's velocity is always *exactly* three times smaller than the thief's (preserving an appropriate direction).

Here is the complete list of the watcher's guarding capabilities:

- (a) if the thief enters $E-A-F$ through E , he cannot escape through F
- (b) if the thief enters $E-A-F$ through F , he cannot escape through E
- (c) if the thief enters $D-B-F$ through D , he cannot escape through F
- (d) if the thief enters $D-C-E$ or $D-E$ through D , he cannot escape through E

As we already know, *the chaser* forces the thief to switch between nodes D , E , and F . Now, the conditions (a)–(d) impose strict restrictions on the order in which the thief can visit these nodes:

- only node D can be visited directly after E or F ,
- only node F can be visited directly after D , and this can only be done via edge $D-F$.

These limitations are illustrated by a directed multigraph in Fig. 4. It turns out that the policemen are able to force the thief to run in the cycle $D \rightarrow F \rightarrow D$. But how can they eventually catch him? It is enough to provide one more instruction to the chaser: he must traverse the edges of the triangle DFB only clockwise.

This does not change his ability to keep the thief moving and make him change the nodes, but in this way he will eventually bump into the thief when he is already forced to run in cycle. This completes the proof that the policemen have a winning strategy in this case.

Now we prove that for $\kappa > 3$, it is the thief who has a winning strategy (with a proper initial placement). This is already suggested by the previous analysis. Basically his strategy is to start at one of the nodes D , E , F and move to another of those nodes whenever he is threatened by one of the policemen. Let us work out the details.

Assume that the thief starts at node D . He stays there until one of the policemen (whom we call the chaser again) gets closer to him than, say, $\varepsilon = 0.2$ (we assume $|EF| = 1$). Then the thief attempts to move to either E or F . Without loss of generality assume that the chaser approaches the thief from the direction of points B or F . Assume that the thief covers length 1 in one minute. Consider the following cases:

- (I) If the other policeman prevents the thief from going directly to F , then there is no policeman on edge $D-E$ and hence the thief can reach E in one minute – less than is needed for both policemen to get there (Fig. 5).
- (II) If the other policeman is on edge $D-E$ then the thief can reach F in two minutes, and he gets there any policeman arrives (Fig. 6). Note that if the chaser is on segment BD , the thief can reach F in just one minute, but this is not important for our analysis.
- (III) Otherwise the thief can directly reach E in 1 minute and F in at most 2 minutes. Note that it takes more than 2 minutes for the chaser (who initially is close to D) to get to any of the points E or F . As for the other policeman, Figure 7 presents two sets – light blue is the set of points, starting from which he can get to E in 1 minute and light green – the set of points, starting from which he can get to F in 2 minutes. It is clear that by the assumption $\kappa > 3$ those two sets do not intersect. Hence the thief can pick one of those nodes, being sure that he will reach it before the other policeman.

Of course, being able to switch nodes once implies the ability to do so indefinitely. Hence we can conclude that the thief has a winning strategy if and only if $n = 1$ and $\kappa \geq 1$ or $n = 2$ and $\kappa > 3$. Naturally, this problem can be generalized to other village configurations, such as the 2×2 grid or even more difficult ones, such as the $N \times M$ grid. We encourage the reader to explore similar strategies for these cases.

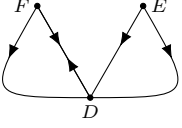


Fig. 4

Note that, contrary to his name, the chaser may be arbitrarily slow. But definitely he needs to be persistent

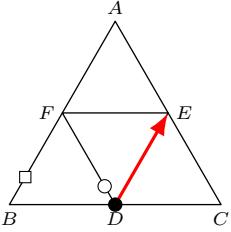


Fig. 5. The thief is depicted by a black circle, the policemen are white circle and square (the chaser is denoted by a circle)

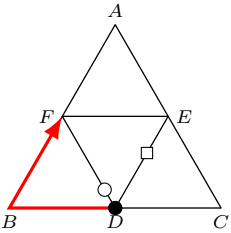


Fig. 6.

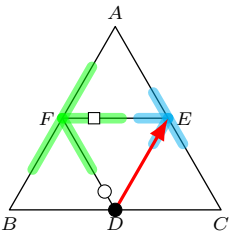


Fig. 7.

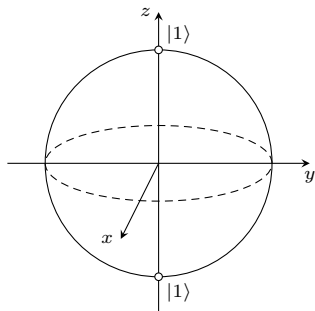
Beyond Classical Limits: The Power and Potential of Quantum Computing

Pranav CHALLA*

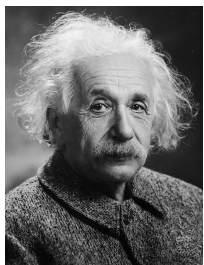
*Student, Queen Elizabeth's School

The world's most common encryption algorithm, RSA encryption, works on the principle that it is difficult to factorize large numbers. However, Shor's algorithm, a quantum algorithm named after Peter Shor, can factorize integers in $O(\log(N)^2)$ time.

All possible states of a qubit can be represented by points on a sphere in three-dimensional space. The poles of the sphere represent the $|1\rangle$ and $|0\rangle$ states, and the *equator* represents states that are in perfect superposition. This representation, known as the Bloch sphere, is named after physicist Felix Bloch.



The concept of particles having an effect on each other from a distance is counterintuitive, even to Albert Einstein, who referred to quantum entanglement as “spooky action at a distance.”



Imagine a computer that could break codes that would usually take millions of years to crack in seconds. Imagine a computer that could process multiple possibilities simultaneously. Quantum computing makes this possible by leveraging the laws of quantum mechanics—the fundamental rules that govern the behavior of the smallest particles—and manipulating their strange properties to increase computational speed to levels incomprehensible for classical computers.

Two key quantum properties that I will explore are *superposition* and *entanglement*.

Superposition

While classical computers rely on bits that exist in a state of 0 or 1, quantum computers use qubits (quantum bits), which can exist in a state of 0, 1, or both simultaneously, thanks to the phenomenon of superposition. To understand this concept, we can explore the mathematics behind it. A quantum state can be written as:

$$|\psi\rangle = \alpha|0\rangle + \beta|1\rangle.$$

Where α and β are complex numbers, normalized such that $|\alpha|^2 + |\beta|^2 = 1$. Here, $|\alpha|^2$ and $|\beta|^2$ correspond to the probabilities of the qubit being in the $|0\rangle$ and $|1\rangle$ states, respectively.

For example, the state $|\psi\rangle = \frac{1}{\sqrt{2}}|0\rangle + \frac{1}{\sqrt{2}}|1\rangle$ corresponds to the qubit being equally likely to be either in the $|0\rangle$ or $|1\rangle$ state when measured.

The concept of superposition is fundamental to quantum computing, as it allows for parallel processing. Since one qubit can hold information about two states at once, two qubits in superposition can represent four states ($|00\rangle$, $|01\rangle$, $|10\rangle$, and $|11\rangle$), and n qubits can represent 2^n states simultaneously. This allows for more efficient search algorithms, such as Grover's algorithm, which can search through N unsorted items in \sqrt{N} searches on average, breaking the classical computing limit of N searches for a list of unsorted items.

Grover's algorithm works using a process known as *amplitude amplification*.

Imagine we have a set of 32 items, with one marked as the correct item. Initially, a superposition of 5 qubits is set up, with each of the 32 output states corresponding to one of the items. Then, a set of quantum operators is applied to increase the probability of the correct item being chosen. This process is repeated until all 5 qubits reflect either the $|1\rangle$ or $|0\rangle$ state, corresponding to the correct item.

Entanglement

Quantum entanglement is the property of quantum particles to become linked. When two quantum particles are entangled, information about one particle provides information about the other. A good analogy is a pair of shoes. Imagine you take each shoe from a pair and place them in separate boxes. By checking one box, you can tell whether the shoe is left or right, but you also know whether the other shoe in the other box, which you haven't opened, is left or right. You gain information about the other shoe without opening the box. The difference is that shoes cannot be in superposition of different states, but qubits can.

For example, consider a state of two qubits, which is a superposition of states $|00\rangle$ and $|11\rangle$ with equal probabilities. So, we know that both qubits are in the same state, but we do not know if it is 0 or 1. This state is described by:

$$|\psi\rangle = \frac{1}{\sqrt{2}}(|00\rangle + |11\rangle).$$

It turns out that this state is entangled. If we measure the first qubit and find it in the state $|0\rangle$, then we can be sure that the second qubit will also be

In 2012, researchers achieved quantum teleportation over a distance of 143 km, from La Palma to Tenerife
arXiv:1205.3909 [quant-ph].

The world's largest quantum computer is a 1,180-qubit system developed by Atom Computing. Each qubit is a neutral atom that is trapped and controlled by an array of lasers.

in $|0\rangle$. Similarly, if the first qubit is found in $|1\rangle$, the second qubit will also be in $|1\rangle$. This correlation holds regardless of the distance between the qubits and enables a level of coordination that classical bits cannot achieve. This means the probability of observing the states $|01\rangle$ or $|10\rangle$ is 0.

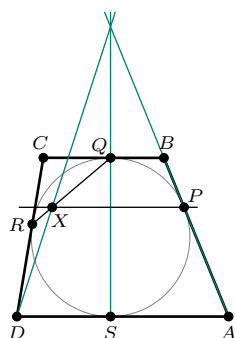
Applications of entanglement are widespread in quantum algorithms. For example, quantum entanglement enables superdense coding, a quantum algorithm that aims to transmit a number of classical bits of information using fewer qubits. Another application of entanglement is quantum teleportation. This theoretical process allows for information transfer through entangled particles. In this process, two parties—located at any distance from each other—use a shared entangled state to transfer information about a given quantum state from one location to another. This process is referred to as the teleportation of a quantum state.

Current Quantum Technology

Quantum technology is still in its early stages, but there has been significant progress. Large tech companies like Google, IBM, and Intel are building computers with increasingly more qubits; however, they are struggling to reduce error rates. Currently, we have noisy intermediate-scale quantum (NISQ) devices, which have enough qubits to perform certain quantum computations but are prone to errors and decoherence (the loss of quantum information). Scientists are working on developing error-correction techniques and „quantum error-correcting codes” to reduce decoherence. The ultimate goal is to build error-resistant quantum computers with applications across various industries. Large-scale quantum computers may still be a decade away, but the current pace of innovation suggests a bright future for quantum technology.



Problems



Edited by Dominik BUREK

M 1813. Let $ABCD$ be a trapezoid ($DA \parallel CB$) circumscribed on a circle that is tangent to the sides AB , BC , CD , and AD at points P , Q , R , and S , respectively. A line passing through P and parallel to the bases of the trapezoid intersects the line QR at point X . Prove that the lines AB , QS , and DX intersect at a single point.

M 1814. Given numbers a , $b > 1$, for which

$$a + \frac{1}{a^2} \geq 5b - \frac{3}{b^2}.$$

Prove that

$$a > 5b - \frac{4}{b^2}.$$

M 1815. Consider two integers $n > 20$ and $k > 1$ such that $k^2 | n$. Prove that there exist positive integers a , b , and c such that

$$n = ab + bc + ca.$$

Edited by Andrzej MAJHOFER

F 1117. In a tightly sealed cylinder, under the piston, there are $m = 10$ g of liquid water. A very rapid movement of the piston causes the pressure in the cylinder to drop to nearly zero. The surrounding temperature and the cylinder with water are at 0°C . How much ice will be produced as a result of this process? It can be assumed that initially, under the piston, there was only liquid water. The latent heat of fusion of water is $L_f \approx 334$ J/g, and the latent heat of vaporization is $L_v \approx 2260$ J/g.

F 1118. In a sealed container, there is a mixture of helium and neon. The mixture is in thermodynamic equilibrium, with the number of moles of neon and helium being the same. A very small hole is made in the wall of the container. What will be the composition of the gas beam escaping from the container just after the hole is made? In atomic mass units, the atomic masses are: helium $\mu_{\text{He}} = 4$, and neon $\mu_{\text{Ne}} = 20$.

Solutions on page 24

A few different proofs of the Fermat theorem on sum of two squares

Maryna SPEKTROVA*

*Student, University of Cambridge

Let us begin by presenting the well-known theorem – the main subject of this article.

Theorem (Fermat’s theorem on the sum of two squares). *An odd prime number p can be expressed as a sum of two squares if and only if $p \equiv 1 \pmod{4}$.*

The notation $n \equiv l \pmod{k}$ means that $n - l$ is divisible by k . In other words, n and l leave the same remainder when divided by k .

One of the most intriguing aspects of this theorem is the vast number of different proofs, connected to various fields of mathematics. In particular, it can be proved using Gaussian integers, finite and infinite continued fractions, Thue’s lemma, the method of infinite descent, and more. In this article, we present three proofs: two geometric interpretations and one proof based on approximation theory.

Remark. Since for any integer x , it holds that $x^2 \equiv 0, 1 \pmod{4}$, no number congruent to 3 modulo 4 can be represented as the sum of two squares. Therefore, we will only prove one implication.

First Proof

This proof will be based on a lemma concerning parallelogram grids. We do not define this concept formally but instead illustrate an example in the margin.

Lemma (Minkowski’s Lemma). *Consider a parallelogram grid and a convex figure Φ , which is centrally symmetric with respect to the origin. Suppose that $S(\Phi) > 4S_0$, where S_0 is the area of the fundamental parallelogram, and $S(\Phi)$ is the area of Φ . Then, Φ contains a point with integer coordinates in this grid, different from the origin.*

Consider a parallelogram grid defined by the vectors $\vec{u} = (1, m)$ and $\vec{v} = (0, p)$, where m is an integer such that $p \mid m^2 + 1$. The existence of such an m for $p = 4k + 1$ follows from Wilson’s theorem, as shown in the margin.

Now let’s apply Minkowski’s lemma to the circle with the center in the origin and the radius $\sqrt{2p}$. As $S(\Phi) = 2\pi p > 4p = 4S_0$, we obtain a lattice point A inside this circle, which in the basis (\vec{u}, \vec{v}) has integer coordinates (x_0, y_0) . Thus, the Cartesian coordinates of A are given by

$$x_0 \cdot \vec{u} + y_0 \cdot \vec{v} = (x_0, mx_0 + py_0).$$

The squared distance of A from the origin is

$$x_0^2 + (mx_0 + py_0)^2 = x_0^2 + m^2 x_0^2 + 2mx_0 py_0 + p^2 y_0^2 = x_0^2(m^2 + 1) + p(2mx_0 y_0 + py_0^2),$$

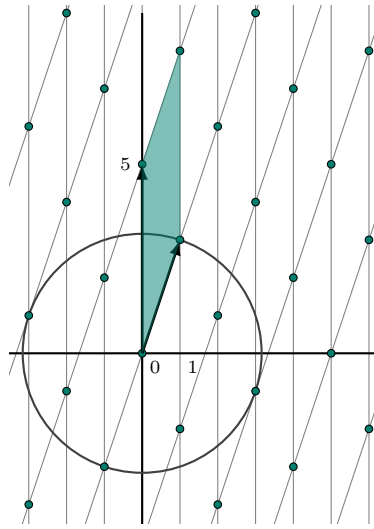
which is divisible by p . Since A lies inside the circle of radius $\sqrt{2p}$, this value is in the open interval $(0, 2p)$, so it must be equal to p . Therefore, the two squares we are looking for are x_0^2 and $(mx_0 + py_0)^2$. \square

Second proof

This proof is often referred to as the “one-sentence proof by Don Zagier”, and indeed, when first published in 1990, it contained only one sentence. For better readability, we present it here in a slightly more detailed form.

Consider the set S containing all triples (x, y, z) of natural numbers that satisfy $x^2 + 4yz = p$. Clearly, for each prime p , the set S is finite. Let us define the following function $f : \mathbb{N}^3 \rightarrow \mathbb{N}^3$:

$$f(x, y, z) = \begin{cases} (x + 2z, z, y - x - z), & \text{when } x < y - z, \\ (2y - x, y, x - y + z), & \text{when } y - z < x < 2y, \\ (x - 2y, x - y + z, y), & \text{when } 2y < x. \end{cases}$$



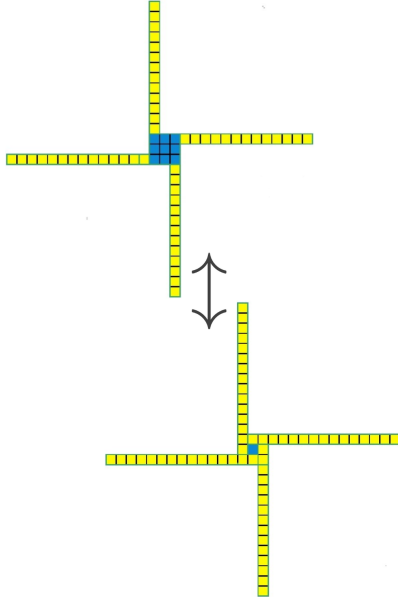
An example of the grid given by vectors $(0, 5)$ and $(1, 3)$.

We will identify a natural number m satisfying $p \mid m^2 + 1$. We use Wilson’s theorem, which states that $(p-1)! \equiv -1 \pmod{p}$ for any prime p . From this theorem, it follows that $-1 \equiv (p-1)!$

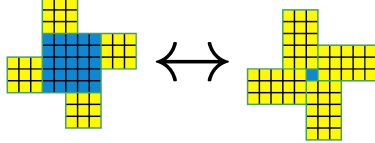
$$\begin{aligned} &= 1 \cdot 2 \cdot \dots \cdot \left(\frac{p-1}{2}\right) \cdot \left(\frac{p+1}{2}\right) \cdot \dots \cdot (p-1) \\ &\equiv 1 \cdot 2 \cdot \dots \cdot \left(\frac{p-1}{2}\right) \cdot \left(-\frac{p-1}{2}\right) \cdot \dots \cdot (-1) \\ &= \left(\left(\frac{p-1}{2}\right)!\right)^2 \cdot (-1)^{\frac{p-1}{2}} \\ &= \left(\left(\frac{p-1}{2}\right)!\right)^2 \pmod{p}. \end{aligned}$$

The last step holds because $p \equiv 1 \pmod{4}$. Thus, $p \mid m^2 + 1$ for $m = \left(\frac{p-1}{2}\right)!$.

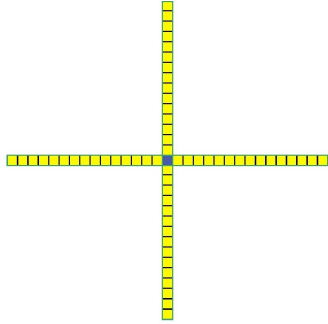
Wojciech Czerwiński wrote about Zagier’s proof in Δ_{17}^7 .



Example of the involution for $p = 61$
 $((3, 1, 13) \leftrightarrow (1, 15, 1))$



Example of the involution for $p = 61$
 $((5, 3, 3) \leftrightarrow (1, 3, 5))$



The only fixed point of f for $p = 61$ is
 $(1, 1, 15)$. Observe how this configuration
differs from $(1, 15, 1)$

Wojciech Czerwiński wrote about
Dirichlet's approximation theorem in
Delta 3/21.

We will refer to the triples appearing in the respective cases of f as first, second, and third type triples.

By performing straightforward calculations, we can easily verify that:

- $f(S) \subseteq S$;
- f is a bijection and, in fact, an involution, meaning that $f(f(x, y, z)) = (x, y, z)$;
- Triples of the first, second, and third type map respectively to triples of the third, second, and first type.

Now, let us investigate which triples $t \in S$ are fixed points, i.e., satisfy $f(t) = t$. A triple can be a fixed point only if it is of the second type, which leads to the following system of equations:

$$\begin{cases} 2y - x = x, \\ y = y, \\ x - y + z = z, \end{cases}$$

which simplifies to $x = y$. We know that $x^2 + 4yz = p$, so $x^2 + 4xz = p$. Since p is a prime number, we easily obtain $x = y = 1, z = \frac{p-1}{4}$, meaning that there is exactly one fixed point in S . This implies that S has an odd number of elements.

Observe that we can pair the elements of S such that each triple (x, y, z) is paired with (x, z, y) . Since S has an odd number of elements, at least one triple must be paired with itself. For this triple (x_0, y_0, z_0) , we have $y_0 = z_0$, so $p = x_0^2 + 4y_0^2 = x_0^2 + (2y_0)^2$. \square

An intriguing aspect of this proof is the geometric interpretation of the function f , surprisingly published only in 2007. For each triple in S , we can consider a square with side x and attach four rectangles with sides y and z to it, as shown in the diagram. Each such figure (a “mill” or “square with wings”) can be obtained by two different cuts: one forming a smaller square and one forming a larger one. Thus, we obtain an involution between all triples in S (which in fact is just f), with crosses as fixed points. Since for a cross-shaped figure, p must be divisible by the side of the main square, this side must be equal to 1. Thus, there is exactly one fixed point. Now, the same reasoning as above completes the proof.

Third proof

This proof is based on the following theorem, which intuitively describes how well we can approximate a given real number by rational numbers with denominators not exceeding a given integer N .

Theorem (Dirichlet's approximation theorem). *For every $\alpha \in \mathbb{R}$ and $N \in \mathbb{N}$, there exist $r, q \in \mathbb{Z}$ such that:*

- $1 \leq q \leq N$, and
- $|\alpha - \frac{r}{q}| \leq \frac{1}{Nq}$.

Now consider such an m that $p \mid m^2 + 1$, and apply Dirichlet's approximation theorem for $\alpha = \frac{m}{p}$ and $N = \lceil \sqrt{p} \rceil$. Then, there exist $q \in \mathbb{N}, r \in \mathbb{Z}$ such that $1 \leq q \leq N$ and $|\frac{m}{p} - \frac{r}{q}| \leq \frac{1}{Nq}$, which is equivalent to $|mq - rp| \leq \frac{p}{N} < \sqrt{p}$.

Define M as $(mq - rp)^2 + q^2$. It is easy to check that $M \equiv m^2q^2 + q^2 \equiv 0 \pmod{p}$.

- **Case 1:** $q \neq N$

Since both $(mq - rp)^2$ and q^2 are less than p , we have $0 < M < 2p$. But M is divisible by p , so $M = p$, which gives $p = (mq - rp)^2 + q^2$.

• **Case 2:** $q = N$

It is easy to show that $M < 3p$, so $M \in \{p, 2p\}$. If $M = p$, the theorem is already proved. Now consider the case $M = 2p$. Then

$$(mq - rp)^2 > 2p - (\sqrt{p} + 1)^2 = (\sqrt{p} - 1)^2 - 2,$$

so

$$|mq - rp| \in \{\lfloor \sqrt{p} - 1 \rfloor, \lfloor \sqrt{p} \rfloor\} = \{q - 2, q - 1\}.$$

Moreover, in this case, $|mq - rp|$ and q have the same parity, so $|mq - rp| = q - 2$. Thus, $(q - 2)^2 + q^2 = 2p$, which simplifies to $(q - 1)^2 + 1 = p$, meaning that we have represented p as the sum of two squares. \square

When we compare the first and third proofs, we can notice several similarities. Is this merely a coincidence? It turns out that Dirichlet's theorem can actually be derived from Minkowski's theorem.

To see this, consider the set

$$S = \left\{ (x, y) \in \mathbb{R}^2 : |x| < N + \frac{1}{2}, |y - \alpha x| \leq \frac{1}{N} \right\}.$$

The set S is a parallelogram centered at the origin with area equal to $2(N + \frac{1}{2}) \cdot \frac{2}{N} > 4$, so we can apply Minkowski's theorem to S on the standard Cartesian lattice. This yields an integer point (q, r) in S (by symmetry, we can take q positive), and these q, r satisfy the condition from Dirichlet's theorem.

Theorem (Jacobi's two-square theorem)

Not only does Fermat's theorem have several surprising proofs, but the same is true for one of its generalizations. The following theorem can be proven using quadratic forms, elliptic functions, or Gaussian integers, but here we present only a proof using generating functions.

Theorem (Jacobi's two-square theorem). *Let $r_2(n)$ denote the number of ways to represent a natural number as a sum of squares of two integers. Moreover, let $d_k(n)$ denote the number of natural divisors of n that leave a remainder k modulo 4. Then, for any natural number n , the following holds:*

$$r_2(n) = 4(d_1(n) - d_3(n)).$$

Remark. *Since for every prime number of the form $p = 4k + 1$ we have $d_1(p) = 2$ and $d_3(p) = 0$, Fermat's theorem follows directly from this one.*

Our proof of this theorem (actually, just a very brief sketch) will be based on the following theorem:

Theorem (Jacobi triple product). *For any complex numbers q and z satisfying $|q| < 1$ and $z \neq 0$, the following identity holds:*

$$\prod_{m=1}^{\infty} (1 - q^{2m}) (1 + q^{2m-1} z^2) (1 + q^{2m-1} z^{-2}) = \sum_{n=-\infty}^{\infty} q^{n^2} z^{2n}.$$

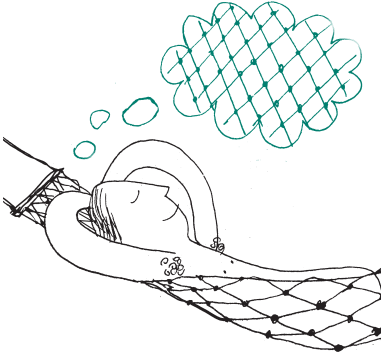
Using this theorem multiple times, the following identity can be proven:

$$\begin{aligned} k^{-1} \prod_{m=1}^{\infty} (1 - x^{4m}) (1 - x^{4m-3} k^2) (1 - x^{4m-1} k^{-2}) \\ + \prod_{m=1}^{\infty} (1 - x^{4m}) (1 - x^{4m-3} k^{-2}) (1 - x^{4m-1} k^2) \\ = \prod_{m=1}^{\infty} (1 - (-x)^m) (1 + (-x)^m k) (1 + (-x)^{m-1} k^{-1}). \end{aligned}$$

Differentiating both sides of this equation with respect to k and substituting $k = -1$, we obtain the following identity:

$$\left(\sum_{n=-\infty}^{\infty} x^{n^2} \right)^2 = 1 + 4 \sum_{n=1}^{\infty} \left(\frac{x^{4n-3}}{1 - x^{4n-3}} - \frac{x^{4n-1}}{1 - x^{4n-1}} \right).$$

There are actually several directions in which Fermat's theorem may be generalized or expanded: one can look on the primes of the form $x^2 + ny^2$, obtain a criterion to all natural numbers to be representable as a sum of two squares (Sum of two squares theorem), consider larger amount of squares (Legendre's three-square theorem, Lagrange's four-square theorem), and so on.



In fact, this equation is equivalent to Jacobi's theorem. To see this, let us first rewrite the right-hand side. The standard formula for the sum of a geometric series implies:

$$\begin{aligned} \sum_{n=1}^{\infty} \left(\frac{x^{4n-3}}{1-x^{4n-3}} - \frac{x^{4n-1}}{1-x^{4n-1}} \right) &= \sum_{n=1}^{\infty} \left(\sum_{k=1}^{\infty} x^{(4n-3)k} - \sum_{k=1}^{\infty} x^{(4n-1)k} \right) \\ &= \sum_{n \in \mathbb{N} \setminus \{0\}, k \in \mathbb{N}} (x^{(4n-3)k} - x^{(4n-1)k}) = \sum_{k=1}^{\infty} (d_1(k) - d_3(k))x^k. \end{aligned}$$

Now let us rewrite the left-hand side:

$$\left(\sum_{n=-\infty}^{\infty} x^{n^2} \right)^2 = \left(\dots + x^{(-1)^2} + x^{0^2} + x^{1^2} + \dots \right)^2 = 1 + \sum_{k=1}^{\infty} r_2(k)x^k.$$

Thus, we have proved that

$$1 + \sum_{k=1}^{\infty} r_2(k)x^k = 1 + \sum_{k=1}^{\infty} (4d_1(k) - 4d_3(k))x^k,$$

which completes the proof of Jacobi's theorem. \square

Paul Erdős, one of the greatest mathematicians of the 20th century, often referred to The Book, where God keeps the perfect proofs for mathematical theorems. He famously said: "You don't have to believe in God, but, as a mathematician, you should believe in The Book". If such a book truly exists, I believe that these proofs, which are an excellent example of the deep connections between different areas of mathematics, would certainly deserve a special place in it.

Can you see a graph here?

*Sylwia SAPKOWSKA**

*Student, Faculty of Mathematics, Informatics, and Mechanics, University of Warsaw

Graph search algorithms are everywhere. Without them, your favorite web search engine wouldn't work, and you probably optimize your own "graph paths" subconsciously – for example, when planning your day. The connections between you, your friends, and your family also form a graph, which we feverishly search through during social gatherings.

Since graph search algorithms have many applications in everyday life, it's no surprise that numerous math olympiad problems can also be solved using this idea.

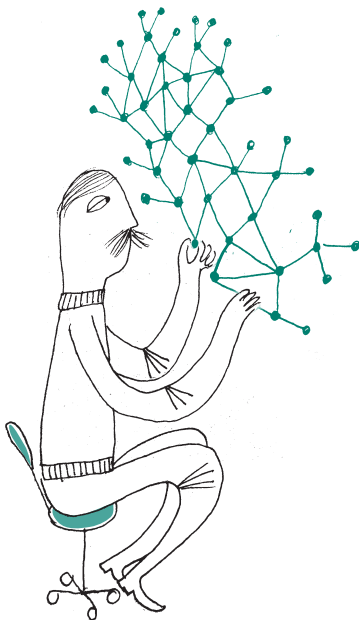
Depth First Search

Before moving forward, let's discuss the simplest graph search algorithm – **Depth First Search**, or DFS for short.

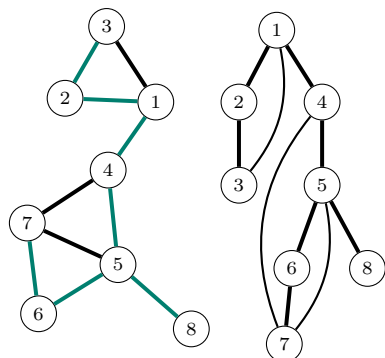
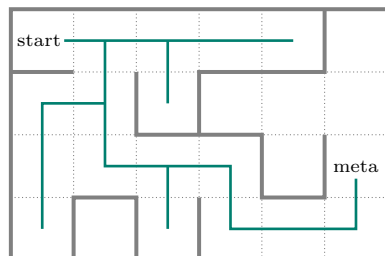
We can think of it as a "walk" through a graph. While performing the algorithm, we keep track of whether a given vertex has already been visited. We start by selecting an initial vertex. When we reach some vertex v during the execution of the algorithm, we follow these steps:

1. Mark vertex v as visited.
2. For each adjacent vertex u of the current vertex v , if u has **not** been visited yet – recursively perform this procedure for u .
3. After exploring all adjacent vertices of v , backtrack to the previous vertex – the one from which we arrived at v .

DFS can be thought of as an analogy to sightseeing. Imagine you're a tourist in a bustling city, holding a map and eager to explore every hidden gem the city



The first version of depth-first search was used in the 19th century by the French mathematician Charles Pierre Trémaux as a strategy for solving mazes, like the one below. The cells of the grid can be interpreted as graph vertices. The edges in the graph represent possible movements, so we connect vertices if and only if the cells they represent are adjacent by their sides.



On the left side of the figure, we have a graph with 8 vertices. Suppose we start our DFS at vertex 1. One possible traversal order could be: $1 \rightarrow 2 \rightarrow 3 \rightarrow 2 \rightarrow 1 \rightarrow 4 \rightarrow 5 \rightarrow 6 \rightarrow 7 \rightarrow 6 \rightarrow 5 \rightarrow 8 \rightarrow 5 \rightarrow 4 \rightarrow 1$. Notice that if there were an edge between 3 and 4, this traversal would have gone from 3 to 4 instead of returning to 2. The edges used to reach unvisited vertices form a spanning tree (these edges are marked in red on the left diagram). The diagram on the right shows the same graph with the rooted spanning tree structure. All additional edges – those not used during DFS traversal – are back edges.

has to offer. You start at a famous museum, soaking in the art and history, then look around for another place you haven't visited yet. If you discover a new café, a charming alleyway, or a historical landmark, you head there next, enjoying the sights and adding them to your "visited" list. When you reach a point where everything nearby has been explored, it's time to backtrack – to return to the last place that had unexplored paths. From there, you continue, uncovering new attractions and moving forward until you've fully explored every possible location. This method of sightseeing ensures that you don't miss anything. By the end of your journey, you will have covered the entire city, leaving no landmark undiscovered and no corner unexplored! The same thing happens in a connected graph – after performing DFS, the entire graph becomes "fully visited."

It's easy to see that during the algorithm's execution, each vertex has three possible states – it is either unvisited (not yet reached by DFS), visited (reached but still being explored), or fully explored (all of its adjacent vertices have been examined).

Back to the Problems

Using the DFS algorithm, we can divide the edges of a graph into **tree edges**, also called spanning edges (those traversed during the walk, forming a rooted spanning tree), and **back edges** (the remaining edges, which complete cycles). It is helpful to think of tree edges as directed downwards and back edges as directed upwards.

Why is this way of analyzing a graph useful? To see this, let's prove the most important property concerning DFS traversal. Suppose we have a connected graph G and perform DFS on it, starting from an arbitrary vertex r .

Our goal is to show that for any edge (u, v) , the vertex v is either an ancestor or a descendant of u in the DFS tree – meaning that v either lies on the path from u to the root r or is in the subtree of u .

Why does this property hold? Suppose there is an edge (u, v) , and without loss of generality, DFS reaches u while v is still unvisited. Then:

- If DFS moves from u to v using (u, v) , then (u, v) is a tree edge.
- If DFS does not proceed to v from u using (u, v) , then v must have already been visited when this edge was considered. This could have happened only if v was reached and explored earlier, during the traversal of some other branch originating from u .

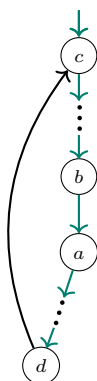
In both cases, v is a descendant of u in the DFS tree.

The key advantage of the DFS tree is that it simplifies graph analysis. Instead of handling various types of edges, we can focus on a tree structure with a few additional edges connecting ancestors to descendants. This makes the graph much easier to analyze.

Problem: Let G be a connected, undirected graph. Prove that the edges of G can be oriented in such a way that the resulting directed graph is strongly connected if and only if G has no bridges, i.e., edges whose removal disconnects the graph.

Solution: If G has a bridge (u, v) , directing this edge from u to v (without loss of generality) means there is no path from v to u . If such a path existed, (u, v) would not be a bridge. Now, let's focus on the other implication.

Assume that G has no bridges. Perform DFS on the graph, starting from an arbitrary vertex r . This process forms a rooted spanning tree using tree edges, along with additional back edges. Let's orient tree edges downward (from the root) and back edges upward (towards the root). To prove that such a graph is strongly connected, we need to show that there exists a directed path from r to



every vertex and, symmetrically, a path from every vertex to r . The first part is easy – since DFS visits every vertex, there exists a path using only tree edges from r to each vertex.

Define the depth of a vertex v as the number of tree edges from the root r to v . Consider a vertex a distinct from the root. In the DFS tree, there is a tree edge (b, a) connecting a to its parent b . Since the graph has no bridges, for the tree edge (b, a) , there must exist some back edge (d, c) connecting some vertex d from the subtree of a (possibly $d = a$) to some ancestor c of b (possibly $c = b$). Otherwise, (b, a) would be a bridge.

To find a path from a to the root, start by traveling from a to d using tree edges. Then, follow the back edge from d to c . Since the depth of c is smaller than that of a , we repeat this process until reaching the root.

Problem (LXVII Polish Mathematical Olympiad, second stage):

Given a connected, undirected graph with an even number of edges, prove that its edges can be paired in such a way that each pair shares exactly one common vertex (in other words, each pair forms a path of length two).

Solution: Perform the DFS algorithm on the graph starting from an arbitrary vertex r and define the depth of a vertex v as the number of tree edges from the root r to v . We will now describe an algorithm for processing the vertices. After pairing two edges, we can remove them. Initially, all vertices are marked as unprocessed:

- Select an unprocessed vertex v with the greatest depth that is not the root.
- Consider the edges from v that have not yet been removed. There are three types of such edges:
 - back edges connecting v with its ancestors,
 - tree edges connecting v with its children,
 - a single edge connecting v with its parent via a tree edge.
 If the number of remaining edges is even, we pair them arbitrarily and remove all of them. Otherwise, we pair them in such a way that only the edge from v to its parent remains.
- Mark v as processed.

It remains to pair up the edges outgoing from r . There is only one type of such edges – those connecting r to its children. Initially, the graph had an even number of edges, and each removed pair consisted of exactly two edges. Thus, r has an even number of children, and we can pair them arbitrarily.

Now, we should discuss why this construction is correct. When considering a vertex v , the vertices in its subtree are already processed. Since in one step of the algorithm we remove all children of a vertex, the only remaining edges in the subtree of v before pairing must be precisely its children, and they will certainly be paired when processing v .

On a Special Vertex in Trees

Everyone knows what trees are. They grow in parks (somehow upside-down – why is the root at the bottom?). Usually, such trees grow symmetrically in every direction – rarely does one branch have noticeably more leaves than others. Is this also the case with graph trees? It turns out that the answer is yes. More formally, we will show that in every tree with n vertices, there exists a vertex v such that if we root our tree at v , then each of its subtrees has size at most $\lfloor \frac{n}{2} \rfloor$. Any such vertex is called a **centroid** or a **tree center**.

We will attempt to find such a vertex recursively. Suppose we root our tree at some vertex r . If all subtrees of r have sizes at most $\lfloor \frac{n}{2} \rfloor$, then we are done, as we have found a vertex with the desired property. Otherwise, there must be a vertex w that is a child of r whose subtree has size greater than $\lfloor \frac{n}{2} \rfloor$. Moreover, such a vertex must be unique – if there were at least two subtrees with sizes



$s_1, s_2 > \lfloor \frac{n}{2} \rfloor$, then we would have:

$$n \geq s_1 + s_2 + 1 \geq 2 \left(\left\lfloor \frac{n}{2} \right\rfloor + 1 \right) + 1 > n,$$

which contradicts the total size of the tree. Similarly, we can show that if the subtree of w has size greater than $\lfloor \frac{n}{2} \rfloor$, then after rooting the tree at w , the subtree containing r will have size at most $\lfloor \frac{n}{2} \rfloor$.

Thus, we can traverse through all neighbors of r , and since w is unique, we recursively check whether w is a suitable candidate for a centroid. This algorithm must terminate because, in each step, the size of the largest subtree decreases.

Observe that a centroid is not necessarily unique. For example, in a graph consisting of two vertices connected by an edge, both vertices are centroids – each of them has a subtree of size $1 = \frac{2}{2}$. From this example, we can conclude that a tree has exactly two centroids if and only if there exists an edge whose removal splits the tree into two smaller trees, each with exactly $\frac{n}{2}$ vertices (the proof is left as an easy exercise).

Problem: Assume that in a certain country where the MBL camp will be held, there are n cities connected by $n - 1$ roads forming a tree. As the organizer of the camp, your task is to efficiently accommodate the participants. Exactly $2k$ people from different cities v_1, \dots, v_{2k} have been admitted. During the camp, participants will form pairs (teams of two friends). The pairing has not yet been determined. Each pair will require accommodation. There is exactly one hotel in each city. Participants from the same pair should stay in the same hotel (and there may be other pairs in that hotel as well). The condition that must be met is as follows: if people from cities u and w form a pair, their hotel must be located in a city on the shortest path connecting u and w (possibly in u or w). Since renting many hotels in different cities would be an organizational challenge, pair up the participants in a way that minimizes the number of different hotels used while satisfying the above condition.

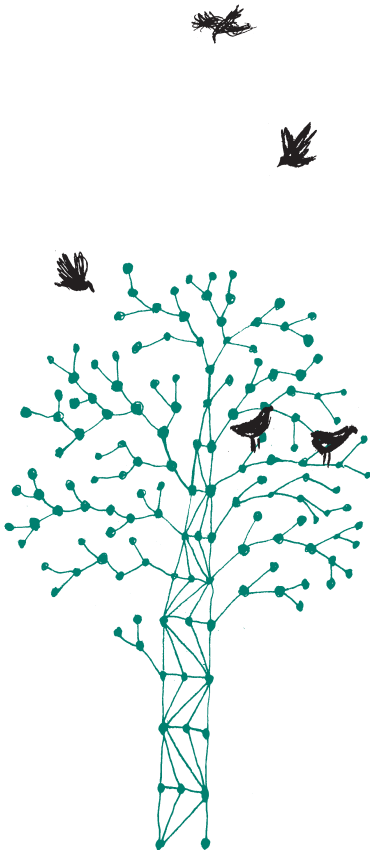
Solution sketch: In this problem, we are given a tree with $2k$ special vertices $W = \{v_1, \dots, v_{2k}\}$. Let's assign a weight to each vertex: $c_v = 1$ if $v \in W$ and 0 otherwise. If we find a vertex v such that in every subtree formed by removing v , there are at most k special vertices, then the problem is solved. Why? Because we can then greedily pair up vertices from different subtrees with the highest number of special points, and such paths will always pass through v . The question remains: how do we find such a vertex v ? The definition of v resembles the definition of a centroid. Instead of calculating subtree size, we will compute the sum of weights in the subtree. Then, the centroid-finding algorithm will also find our desired vertex v . Therefore, we conclude that it is always sufficient to rent just one hotel.

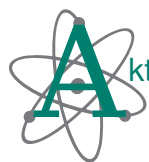
Here is another problem, this time left as an exercise for the reader:

Problem (based on a task from the second stage of the XXX Polish Olympiad in Informatics): Antek and Marysia are playing a game on a tree. Initially, all vertices are white, except for one vertex x , which is colored red (belonging to Antek), and another vertex y , which is colored blue (belonging to Marysia). Each player takes turns selecting any vertex u of their color and then coloring an adjacent white vertex v with their color. The player who cannot make a move loses the game. Determine who has a winning strategy depending on the initial positions x and y of Antek and Marysia.

Summary

As we have seen, there are many applications of DFS and centroids in mathematical olympiad problems. However, DFS is much more than that – we use graph search algorithms almost constantly without even realizing it! So next time you are solving a sudoku puzzle or rushing to school or work, remember that you are actually recursively following some path in a graph, hoping to find the right way out.





On how some discoveries in various fields of science sooner or later found practical applications (often in very unexpected ways), we wrote in issue Δ_{19}^{11} .



Raw



Hard-boiled



Soft-boiled



Sous vide



Periodic

Soft-boiled, hard-boiled... and just right

Scientists engaged in fundamental research are occasionally faced with the necessity of answering questions about how the results of their studies will be applied in so-called 'everyday life.' It is well known that not all research yields results that can be immediately applied in industry, gastronomy, or entertainment.

One may wonder whether the goal of a certain group of researchers from Naples, Italy, was indeed to find an application for mathematical modeling methods and advanced imaging techniques in everyday life, or whether the inspiration came from an entirely different source. Regardless of their motivation, there is no doubt that the task they set for themselves was very ambitious. It might seem that the topic of cooking eggs has already been thoroughly and exhaustively explored by humanity through experiments repeated billions of times, leaving nothing new to be discovered. Everyone knows hard-boiled and soft-boiled eggs. It is common knowledge that for a hard-boiled egg, it should remain in boiling water longer, whereas for a soft-boiled egg, it should be cooked for a shorter time. Exactly how long this 'shorter' duration should be depends on personal preferences, and acquiring this knowledge requires some practice, but determining the optimal cooking time is relatively straightforward after a few trials.

It turns out that sometimes reading a scientific article can expand our culinary horizons. In the paper [1], the aforementioned group from Naples compares a new egg cooking method proposed by them with three previously known methods. What is this third method (apart from *hard-boiled* and *soft-boiled*)? Perhaps some Readers are already familiar with it, but no one in the *Delta* editorial team had heard of it before. It is called *sous vide* or $6X^{\circ}\text{C}$ and involves cooking eggs at a temperature between 60°C and 70°C for at least an hour. This relatively new but apparently increasingly popular method produces a very specific result—both the egg white and the yolk acquire the same creamy consistency.

This form of egg preparation likely has its enthusiasts; however, not everyone appreciates that albumen in this method does not fully set, as some proteins in the white solidify at temperatures higher than 70°C . The albumen and yolk have two very different compositions and consequently require different temperatures to reach their optimal states. The white would ideally cook at 85°C , while the yolk at 65°C .

A solution to the problem of different optimal temperatures could be to break the egg and prepare the white and yolk separately. But what if we insist on cooking the egg whole, in its intact shell? This is where the proposal from the Naples researchers comes in: the egg should be alternately placed in boiling (100°C) and cold (30°C) water. The switching should occur every 2 minutes, and a total of 8 cycles should be performed, meaning the entire process should last 32 minutes. The authors have named this method *periodic cooking*. The cooking time and switching frequency were determined through numerical simulations, taking into account heat conduction and the energy required for protein denaturation in both the egg white and yolk. In these conditions, the temperature at the egg's center changes slowly and approaches the optimal temperature for cooking the yolk without exceeding it. Meanwhile, closer to the shell, the temperature fluctuations are greater but oscillate around a higher value, optimal for cooking the white.

The numerical simulation predictions were tested experimentally, and according to the authors, they were fully confirmed. Periodically cooked eggs supposedly have an optimal consistency throughout their entire volume. Anyone with 32 minutes to spare can switch an egg between warm and cold water 8 times and then taste it to form their own opinion on whether modern scientific methods truly have applications in gastronomy.

Szymon CHARZYŃSKI

[1] Di Lorenzo, E., Romano, F., Ciriaco, L. et al., 'Periodic cooking of eggs,' *Communications Engineering* 4, 5 (2025).
doi.org/10.1038/s44172-024-00334-w.



First and Foremost: Laughter

How wonderful it is that there is one day in the year when joking is mandatory. Because even if forced, laughter is healthy, and this truth applies not only to humans.

All people on Earth, regardless of their origin and culture, laugh in a similar way. We can unmistakably identify laughter among a wide range of behaviors – despite language barriers and physical differences. We begin to laugh (producing sounds known as laughter) at about 3 months old, and we continue laughing throughout our lives, doing so far more often than we realize.

The positive effects of laughter on health have been known for centuries. Nowadays, more and more information is available about specific changes in the human body that occur when we have a good laugh.

Rapid expulsion of air caused by muscle contractions improves lung ventilation, muscles contract and relax. In the brain, the reward center is activated, and the endorphins released have pain-relieving effects, while growth hormone is secreted. The levels of stress hormones, cortisol and epinephrine, decrease, thereby protecting blood vessels and the heart from the effects of stress.

However, if we were to look at it entirely from the outside, laughter is a strange phenomenon. The loud, high-pitched sounds that accompany it are hardly human. The face distorts, the jaw drops loosely, the body bends and bounces. A sudden burst of laughter takes control: over posture, the ability to perform most activities, speech, and breathing. One can reel from laughter, fall off a chair, cry, develop a sore throat and stomach ache. One might even wet themselves. It is even possible to die laughing. Overall, this behavior is quite dangerous; however, it has been strongly ingrained in the evolutionary process. Where did it come from?

Charles Darwin, in his book 'The Expression of the Emotions in Man and Animals' from 1872, devoted considerable attention to laughter. He described laughter as a state in which the eyes become *bright and sparkling*. Darwin visited the London Zoo, where he observed great apes being tickled by their caretakers. Chimpanzees, bonobos, gorillas, and orangutans have ticklish spots and react to them in a strikingly similar way to humans—also with a kind of laughter, resembling loud and rapid panting.

But not only apes can laugh. In the 1990s, it was discovered that rats have ticklish spots on their backs and bellies. Further research revealed that tickled rodents emit short squeaks in a frequency range inaudible to humans (50 KHz). Rats willingly submitted to tickling, and they greeted the researcher entering the laboratory with their laughter-like chirping.

The described sounds are also made by rodents during play, including interactions with humans. By studying rat vocalizations and ticklish spots, researchers even taught rats to play hide-and-seek. Both the animals and the scientists took turns being the seeker and the hider. It turned out that rats mastered the game brilliantly and were eager to play, even though the reward was belly tickling rather than, as is usual in animal research, a treat. When the rodents hid, they remained completely silent, only emitting joyful squeaks once found by a human. However, these squeaks were absent when the hider did not follow the game's rules, such as always hiding in the same spot.

Scientists believe that human laughter originates from play-related behavior, evolving from loud panting. All young mammals play, and some species retain this ability throughout life. Play-related vocalizations have also been observed in some bird species. Laughter (specific sounds) and body posture, as well as facial expressions, signal an invitation to play and convey the message: what is about to happen is not serious—let's have fun. Play serves as a way to train physical skills in a safe environment and as a means to build social relationships, making it particularly important in social species.



In animals, laughter only occurs during direct physical contact, such as tickling or play (wrestling, rolling, nibbling, etc.). Human laughter, however, is unique in several ways. Humans have a sense of humor and laugh not only during play; they find images, situations, and words amusing. Additionally, only in humans is laughter contagious.

Everyone has likely experienced the dreadful feeling of being overcome with uncontrollable laughter at the most inopportune moment, such as during a solemn ceremony, and being utterly unable to suppress a completely senseless giggle. This affects everyone, even professionals like radio and television announcers. It serves as a way to relieve tension, originates from the oldest regions of our brain, and is very difficult to control. One person's laughter can easily spread within a group, as the brain loves laughter. Studies show that when we hear laughter, we enter a state of readiness—and we start laughing, often without even knowing why.

Although we believe we laugh when something is funny, research indicates that we laugh 30 times more often in company. Laughter is an evolutionarily ingrained, powerful tool for shaping social relationships. Through laughter in conversations, we express sympathy, understanding, and a sense of belonging. We invite listeners to engage, signaling good intentions. Shared laughter helps navigate difficult situations, relieve tension, and strengthen bonds.

Recently, the world has not been particularly conducive to laughter. In times of frustration and uncertainty, one day a year is not enough. Starting today, let's take laughter seriously.

Marta FIKUS-KRYŃSKA



ą Otwarty 2°: $14 = 2 \cdot 7$

More about autobiographical numbers can be found in the article by Piotr Zarzycki and Ryszard Kubiak, *On Autobiographical Numbers*, Δ_{20}^{12} .

The problem under consideration can be extended to numbers containing the digit 0 in their decimal representation—for example, by assuming $p_0 = 1$, which results in ignoring every occurrence of this digit. Alternatively, one could explore this property in different numeral systems. The final question regarding the total count of numbers possessing this property remains open in these variations as well.

I personally verified that a fifth such number does not exist among numbers with up to 23 digits. However, I am not the record holder in this regard, as indicated by information in the *OEIS* encyclopedia—the sequence is listed under A097227. As it turns out, a much larger range was checked by Chai Wah Wu, an American researcher from IBM.

Bartłomiej PAWLIK

Silesian University of Technology

A few years ago, recreational mathematics found its way under snowy rooftops thanks to a curious property of the number 2020. Specifically, the first digit of this number indicates the count of the digit 0 in its decimal representation, the second digit represents the count of the digit 1, while the third and fourth digits correspond to the counts of digits 2 and 3, respectively. Numbers possessing this self-descriptive property are called *autobiographical*. Naturally, the total number of autobiographical numbers is finite, as they can have at most ten digits. There exist precisely seven such numbers, the largest of which is 6 210 001 000.

Let us examine numbers that also, in a certain sense, describe themselves, but their method of self-description is somewhat subtler. First, let us recall the first nine prime numbers:

$$p_1 = 2, p_2 = 3, p_3 = 5, p_4 = 7, p_5 = 11, p_6 = 13, p_7 = 17, p_8 = 19 \text{ oraz } p_9 = 23.$$

The factorization of the number 14 is $14 = 2 \cdot 7$. Notice that 2 is the **first** prime number, while 7 is the **fourth**. Thus, we have:

$$14 = 2 \cdot 7 = p_1 \cdot p_4.$$

Among numbers that do not contain the digit 0, there are three more known cases where each digit in the decimal representation corresponds to a single factor in their prime factorization:

$$154 = 2 \cdot 11 \cdot 7 = p_1 \cdot p_5 \cdot p_4,$$

$$1196 = 2 \cdot 2 \cdot 23 \cdot 13 = p_1 \cdot p_1 \cdot p_9 \cdot p_6,$$

$$279\,174 = 3 \cdot 17 \cdot 23 \cdot 2 \cdot 17 \cdot 7 = p_2 \cdot p_7 \cdot p_9 \cdot p_1 \cdot p_7 \cdot p_4.$$

Unlike classic autobiographical numbers, here there is no natural upper bound on the size of the sought numbers—multiplying n prime numbers together can yield an n -digit number. So, do more such numbers exist? Are there infinitely many, or at least one more? Currently, **we do not know**—and that is unfortunate, because I would love to find out.

Club 44 F



Solution submission deadline: 30 VI 2025

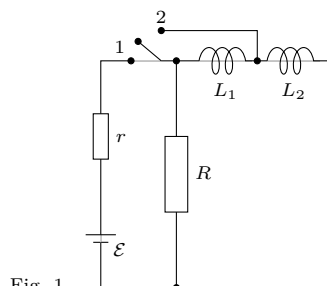


Fig. 1

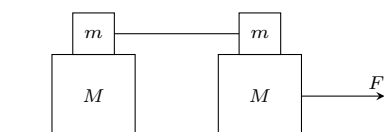


Fig. 2

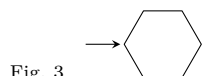


Fig. 3

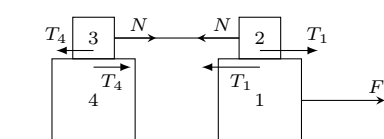


Fig. 4

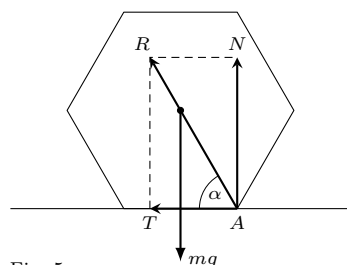


Fig. 5

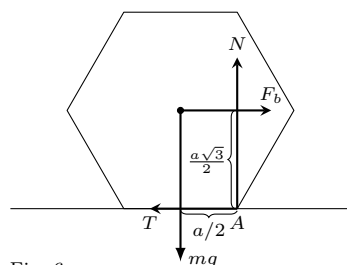


Fig. 6

Leaderboard of the problem-solving league **Klub 44 F** after considering the evaluations of solutions for problems 782 (WT = 1,68), 783 (WT = 3,45) from issue 9/2024

Konrad Kapcia (Poznań)	3–44+3,25
Paweł Perkowski (Ożarów Maz.)	6–44+0,70
Jacek Konieczny (Poznań)	40,87
Tomasz Wietecha (Tarnów)	17–39,17
Jan Zambrzycki (Białystok)	4–28,35
Andrzej Nowogrodzki (Chocianów)	3–27,49

Physics Problems No. 796, 797

Edited by Elżbieta ZAWISTOWSKA

796. In the circuit shown in Figure 1, the switch was closed to position 1, and after the currents stabilized, it was quickly switched to position 2. Assuming that the inductors L_1 and L_2 are ideal, determine the amount of heat dissipated in the resistor R after switching. The electromotive force of the source is \mathcal{E} , and its internal resistance is r .

797. At the center of the bottom of a rectangular barge with a length of $a = 80$ m, a width of $b = 10$ m, and a height of $c = 5$ m, a hole with a diameter of $d = 1$ cm has formed. Estimate the time after which the barge will sink if no water is pumped out. The barge is open at the top, carries no cargo, and the initial height of the hull above the water level is $h = 3,75$ m.

Solutions to problems from issue 12/2024

We recall the problem statements:

788. A system of blocks is placed on a frictionless table, as shown in Figure 2. The coefficient of friction between the blocks of masses M and m is μ . The blocks of masses m are connected by a massless, inextensible string. The lower right block is pulled parallel to the table with a force F . Find the accelerations of all blocks.

789. A hexagonal pencil is pushed along a horizontal surface, as shown in Figure 3. What must be the coefficient of friction μ between the pencil and the surface for the pencil to slide without rotating?

788. The accelerations of the blocks of mass m are the same because they are connected by an inextensible string. The friction between blocks 3 and 4 (Fig. 4) is static friction. If block 3 were to slide on block 4, the friction force between them, $T_4 = \mu mg$, would be smaller than the tension force N , causing block 2 to move left, which is impossible. Therefore, the accelerations of blocks 2, 3, and 4 are equal. Let us denote them as a_2 , and the acceleration of block 1 as a_1 . Two cases are possible:

1) No slipping between blocks 1 and 2, the system moves as a single body:

$$a_1 = a_2 = F/2(M + m).$$

The equation of motion for block 1: $Ma_1 = F - T_1$ and the condition for no slipping $T_1 \leq \mu mg$ allow us to find the condition that the force must satisfy for case one to hold: $F \leq 2\mu mg(M + m)/(M + 2m)$.

2) Block 2 slides on block 1:

From the equation of motion for block 1: $a_1 = (F - \mu mg)/M$.

From the equation of motion for blocks 2, 3, and 4: $a_2 = \mu mg/(2m + M)$.

Case two occurs if the force satisfies the condition:

$$F > 2\mu mg(M + m)/(M + 2m).$$

789. The problem can be solved in a reference frame attached to the surface or the pencil.

1) Inertial frame attached to the surface: The moving pencil experiences two forces from the surface: the normal force N and the friction force T . The pencil cannot move vertically, so the normal force equals the gravitational force $N = mg$, and the friction force is $T = \mu N = \mu mg$. Consider the limiting case when the pencil begins to rotate around edge A (Fig. 5). The forces N and T are applied at edge A . If their resultant force R passes below the pencil's axis, its moment about the axis causes rotation. The condition for no rotation is:

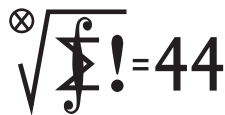
$$\tan \alpha = N/T \geq \tan 60^\circ, \quad \mu \leq 1/\sqrt{3}.$$

2) Non-inertial frame attached to the pencil: In this frame, the pencil experiences an additional fictitious force due to acceleration caused by friction (Fig. 6): $F_b = ma = m\mu g$. The pencil rotates around edge A (instantaneous axis of rotation) if the moment of force F_b about A is greater than the moment of the gravitational force:

$$F_b a \sqrt{3}/2 > mga/2.$$

From this, we obtain the same condition for no rotation as before.

Club 44 M



Submission deadline: June 30, 2025

Top standings in the problem-solving league **Club 44 M** after including scores from problems 885 ($WT = 1,95$) and 886 ($WT = 1,42$) from issue 9/2024

Mikołaj Pater		42.95
Witold Bednarek	Łódź	42.00
Tomasz Wietecha	Tarnów	41.98
Krzysztof Zygan	Lubin	39.38
Andrzej Daniluk	Warsaw	37.89
Andrzej Kurach	Ryjewo	36.18
Michał Warmuz	Zywiec	33.21
Marcin Kasperski	Warsaw	32.31
Jędrzej Biedrzycki		32.29
Krzysztof Kamiński	Pabianice	31.90
Grzegorz Wiączkowski		31.79
Marian Łupieżowiec	Gliwice	31.29

Correction of an editorial error: In the annual summary of the participant list (*Delta* 2/2025), the balance for Grzegorz Wiączkowski should be listed as 29.40.

891. Let $\cos(2^n \varphi) = x_n$ (so $|x_n| \leq 1$). From the cosine doubling formula, we obtain the recurrence relation $x_{n+1} = 2x_n^2 - 1$. We investigate for which initial values x_0 the condition: all $x_n \in [-1, 0]$ is satisfied.

Let $y_n = x_n + \frac{1}{2}$. The problem condition takes the form $|y_n| \leq \frac{1}{2}$, and the recurrence relation transforms into:

$$(1) \quad y_{n+1} = -y_n(2 - 2y_n) \quad \text{for } n = 0, 1, 2, \dots$$

Since $|y_n| \leq \frac{1}{2}$, the expression in parentheses has a value ≥ 1 ; and when $y_n \leq 0$, its value is ≥ 2 . Thus:

$$(2) \quad |y_{n+1}| \geq \begin{cases} |y_n| & \text{for all } n, \\ 2|y_n| & \text{when } y_n \leq 0. \end{cases}$$

From equation (1), it follows that in every pair of consecutive terms of the sequence, there is a non-positive number. From property (2), we now deduce that $|y_{n+2}| \geq 2|y_n|$ for all n . By induction, we obtain $|y_{2n}| \geq 2^n|y_0|$; and since $|y_{2n}| \leq \frac{1}{2}$, we must have $y_0 = 0$. This corresponds to the value $x_0 = -\frac{1}{2}$ (and then all $x_n = -\frac{1}{2}$).

The required condition is therefore satisfied if and only if $x_n = \cos \varphi = -\frac{1}{2}$, which holds only for $\varphi = \pm \frac{2}{3}\pi + 2m\pi$ ($m = 0, \pm 1, \pm 2, \dots$).

892. Solution by the author (Michał Adamaszek). Assume that a player earns 1 point for a win and 0 for a loss. Fix k and let S be the set of players who finished the tournament with k points; let $|S| = s$. Within S , they played $\binom{s}{2}$ matches, so they collectively earned at least

Mathematics Problems No. 899, 900

Edited by Marcin E. KUCZMA

899. Let $g: \mathbb{Z}^2 \rightarrow \mathbb{R}$ be an arbitrary function (\mathbb{Z}^2 is the set of lattice points, i.e., ordered pairs of integers). The distance between points $P, Q \in \mathbb{Z}^2$, where $P = (x, y)$ and $Q = (u, v)$, is defined as $d(P, Q) = \max(|x - u|, |y - v|)$. Prove that there exist infinitely many five-element sets of lattice points $(P_0, P_1, P_2, P_3, P_4)$ such that (for $i = 1, 2, 3, 4$): $d(P_0, P_i) = 1$, $g(P_0) \leq g(P_i)$.

900. Polynomials f_1, f_2, f_3, f_4 of one variable, with real coefficients, satisfy the conditions:

$$f_1(x) \leq f_2(x) \leq f_3(x) \leq f_4(x) \quad \text{for } x \in [0, 1],$$

$$f_2(x) \leq f_4(x) \leq f_1(x) \leq f_3(x) \quad \text{for } x \in [-1, 0].$$

Prove that $f_1 = f_2 = f_3 = f_4$.

Problem 900 was proposed by Mr. Michał Adamaszek from Copenhagen.

Solutions to problems from issue 12/2024

Reminder of the problems:

891. Find all real numbers φ that satisfy the condition: $\cos(2^n \varphi) \leq 0$ for every integer $n \geq 0$.

892. A badminton tournament involves $n \geq 2$ players, where each player competes against every other player once, with no draws. For each $k \in \{0, \dots, n-1\}$, determine the maximum possible number of players who finished the tournament with exactly k wins.

that many points. However, by definition of S , they earned exactly ks points in total. Thus, $\binom{s}{2} \leq ks$, meaning $s \leq 2k + 1$.

Now assume that all match results in the tournament were reversed ($0 \mapsto 1, 1 \mapsto 0$). In this new tournament, S is the set of players who earned exactly $n - k - 1$ points, so the same reasoning gives that $\binom{s}{2} \leq (n - k - 1)s$, meaning $s \leq 2n - 2k - 1$. Therefore,

$$s \leq \min\{2k + 1, 2n - 2k - 1\}.$$

We show that this bound is achievable. In the case when $1 \leq 2k + 1 \leq n$, let S be any set of players of that exact size. It is easy to arrange matches within S so that each player wins exactly k matches (e.g., each player beats k of their successors in any cyclic arrangement of S). Players outside S win all their matches against S and compete arbitrarily among themselves. Then each player in S earns k points, while each player outside S earns at least $2k + 1 \geq k + 1$ points.

In the case when $n + 1 \leq 2k + 1 \leq 2n - 1$, let $j = n - 1 - k$. Then $1 \leq 2j + 1 \leq n - 1$, so by the previous construction, there exists a tournament in which exactly $2j + 1 = 2n - 2k - 1$ players have scored exactly j points. By reversing all results to their opposites, we obtain a tournament in which exactly $2n - 2k - 1$ players have scored exactly k points.

Thus, the desired maximum value of $|S|$ is $\min\{2k + 1, 2n - 2k - 1\}$.

Skrót regulaminu

Anyone may submit solutions to problems from issue n by the end of month $n + 2$. Solution sketches are published in issue $n + 4$. One may submit solutions to four, three, two, or one problem (each on a separate sheet), either every month or with any breaks. Solutions to mathematics and physics problems should be sent in separate envelopes, with the label: **Club 44 M** or **Club 44 F** on the envelope. They can also be sent via email to delta@mimuw.edu.pl (we prefer PDF files). The problems are evaluated on a scale from 0 to 1, with an accuracy of 0.1. The score is multiplied by the difficulty factor of the problem: $WT = 4 - \frac{3Q}{N}$, where S denotes the sum

of scores for solutions to this problem, and N is the number of people who submitted solutions to at least one problem from the given issue in the given category (**M** or **F**)—this is the number of points awarded to the participant. Upon accumulating **44** points, at any time and in either of the two categories (**M** or **F**), the participant becomes a member of **Club 44**, and any excess points are carried over for future participation. Achieving membership three times grants the title of **Veteran**. The detailed rules were published in issue 2/2002 and can also be found on the website deltami.edu.pl.



April is the third consecutive month of the year in which the Sun quickly moves northward, increasing its culmination height by another 10° . After the time change to daylight saving time at the beginning of April, the Sun sets after 7 PM, and by the end of the month, it sets after 8 PM.

The month will begin with a strong highlight, which is the occultation of the Pleiades by the Moon in the 16% phase. On April 1, the Silver Globe will pass through the southwestern part of the cluster, occulting, among others, Electra (17 Tau), Merope (23 Tau), Alcyone (25 Tau), Atlas (27 Tau), and Pleione (28 Tau), as well as the characteristic tail of weaker stars to the south-east of them. Poland will be located at the eastern edge of the occultation zone, so the last two of the mentioned stars cannot be observed as occulted in our country. However, in the case of Merope and Alcyone, their occultation will be visible throughout Poland, but their reappearance will be visible only in the northwestern part of the country. The first of the bright stars of the Pleiades will disappear behind the dark edge of the Moon's disk around 10:45 PM, less than 1.5 hours before the setting of both celestial bodies.

The Moon will remain a decoration of the night sky in the first part of the month. On April 2, its phase will increase to 25% and it will simultaneously approach Jupiter by about 5° . The largest planet of the Solar System can be observed only in the first part of the night. Initially, it will be more than 30° above the western horizon, but as the month progresses and dusk sets in later, the planet will lower its position to less than 15° . During this time, its brightness will drop to -2^m , and its disk diameter to $34''$. On April 16, an interesting configuration of the Galilean moons will occur: in the evening, Ganymede will appear on its disk, and Callisto will pass just to the south of it.

On April 4, Earth's natural satellite will display a half-illuminated disk, and on the following night, it will meet Mars as well as Castor and Pollux in Gemini. Around 9:30 PM, the Moon will occupy a position about 2° north of the Red Planet and simultaneously 3° south of Pollux. Mars will cover 12° on the sky in April, starting the month less than 0.5° from the shining star κ Gem with an observed magnitude of $+3.5^m$, and by the end of the month, it will reach 2° to the open cluster M44 in Cancer. The planet is quickly moving away from us, which will cause its brightness to drop to $+1^m$ by the end of April, and its disk diameter to $6''$. Its phase is still large, nearly 90%, and it can be observed through telescopes.

On the 6th of the month, the Moon will show a 68% phase and will approach the star Asellus Borealis, the northeastern corner of the trapezoid of stars surrounding the already mentioned M44, by less than 0.5° . Two days later, its phase will increase to 85%, and it will be in the central part of the Leo constellation, 3° from Regulus. On the night from April 12 to 13, the Silver Globe will pass through the full moon phase, rising 3° from Spica, the brightest star in Virgo. During the night, the distance between the two celestial bodies will decrease to 1° .

After the full moon, Earth's natural satellite will visit the southernmost part of its orbit, passing deep below the ecliptic. As a result, it will occupy a very low position over the horizon during this time, and on April 18 and 19, it will cross the local meridian even below 10° , making its observations difficult due to terrain obstacles and distortions caused by our atmosphere.

On the night from April 16 to 17, the Moon, at a phase of 86%, will rise around midnight about 1.5° from Antares,

the brightest star in Scorpius. It is worth noting, however, the weaker star τ Scorpii, which will be located 1° to the east of the Moon's disk, as it will disappear for about an hour behind the Moon's disk during the night. This phenomenon can be observed over a small area from the North Sea to the Black Sea, with boundaries at the 60° latitude in the north and the Bulgarian-Greek border in the south. In Poland, the occultation will last from around 3:50 AM to 4:40 AM, and the more interesting end of the phenomenon, occurring at the dark edge of the Moon's disk, will take place under a brightening sky.

On April 21, the Last Quarter Moon will occur, and on the 27th of the month, it will pass through the New Moon phase. Unfortunately, due to the unfavourable inclination of the ecliptic, observations of the Moon at this time will be very difficult. It is quite different in the evening. On April 28, just under a day after the New Moon, a very thin crescent of the Moon in the 2% phase will be visible low over the western horizon. On April 29, the Pleiades will be occulted

again, unfortunately during the daytime, and in the evening, the Moon will appear 7° from them, showing a disk in the 6% phase. To conclude the month, the Silver Globe in the 13% phase will pass 5° north of Jupiter.

As always in the second half of the month, the Lyrids will radiate, with their peak activity around

April 22. The radiant of the shower is located about 8° south-west of Vega and rises at dusk to reach a height of nearly 70° by the end of the astronomical night. At the peak, about 20 events per hour can be expected, and the Moon will not interfere with observations.

Ariel MAJCHER



Straight from Heaven: Again, That Mass Gap

During the first three observational campaigns (O1, O2, and O3), the LIGO-Virgo collaboration registered a total of 90 confirmed gravitational wave signals, but since the start of the O4 campaign, over 200 new signals have already been registered, mostly from the binary black hole systems. This is due, of course, to the improved sensitivity of the detectors and, consequently, the larger volume of the Universe from which signals are reaching us can be observed.

LIGO and Virgo interferometers use triangulation to determine the source's position on the sky. This requires simultaneous detection by at least two, and ideally three, different detectors to compare time differences in the arrival of the gravitational wave and amplitude and phase differences in the signal at each detector. If only one detector is operational, only the arrival time of the signal can be measured, and the amplitude h of the signal can be estimated, i.e., the distance r to the event, because $h \propto 1/r$.

We return to the issue of the 'mass gap,' referring to the hypothetical gap (or void) in the mass distribution of neutron stars and black holes, roughly 3 and $5 M_\odot$ mass gap between the most massive neutron stars and the least massive black holes. We last wrote about it in Δ_{24}^9 , and this time it reappears due to the publication by the LIGO-Virgo-KAGRA (LVK) team. The detection of the interesting GW230529 signal occurred on May 29, 2023, at the beginning of the ongoing LVK O4 observational run (spring 2023 – fall 2025).

The GW230529 signal is particularly interesting because of its source – a binary system – consisted of an object with a mass typical for neutron stars, $1.4^{+0.6}_{-0.2} M_\odot$, and a second object with a mass of $3.6^{+0.8}_{-1.2} M_\odot$, located in the 'mass gap'. Signals from binary systems containing a component in the 'mass gap' have been previously detected by the LIGO and Virgo detectors, but this is the first for which the more massive component lies within it. Due to the fact that at the time of detection, only the LIGO Livingston detector (called L1) was operational, the exact position of the signal on the sky could not be determined. Unfortunately, the second LIGO detector (Hanford, H1) was in the process of being activated, and the Virgo detector (V) was completely offline at the time. As a result, the potential electromagnetic radiation that might have accompanied the final moments of GW230529 could not be observed. Astrophysical models predict the formation of a so-called kilonova, i.e., an explosion of hot radioactive matter after the binary system components collide, or the tidal disruption of a neutron star by a black hole before the final collapse.

The detection of GW230529 is important for many reasons. First, it provides further evidence for the existence of compact objects in the 'mass gap,' an area previously considered to be sparsely 'inhabited.' The question remains, however, about the nature of the more massive component: it is presumably a low-mass black hole, but it is not excluded that it is a very massive neutron star (which would be an extraordinary discovery for researchers studying extremely dense matter). From the analysis of the wave that reached the L1 detector, it appears that the more massive component had a non-negligible spin χ (dimensionless angular momentum $\chi = cJ/(GM^2)$, where J is the angular momentum) estimated at $\chi = 0.44^{+0.40}_{-0.37}$. However, it is not as large as would be expected in the case of a black hole formed from the earlier merger of two smaller black holes. It is estimated that the merger of two smaller, non-rotating black holes leads to the formation of a black hole with a spin $\chi \approx 0.7$, which comes from the transfer of orbital angular momentum of the system to the final spin of the object.

This observation proves that earlier models of stellar evolution and black hole formation processes may need to be refined, as it is already apparent that black holes, especially light ones, can form in many ways, including through neutron star mergers, and perhaps also as a result of explosions of a special class of asymmetric supernovae. It seems more than certain that the 'mass gap' is not a real gap in the mass distribution, but rather a reflection of the current observational limitations. The not entirely successful observation of GW230529 (the failure to detect the phenomenon in electromagnetic waves) is still significant for 'traditional' astrophysics, because now that we have detected GW230529, we will likely detect more events of this type in the future, potentially accompanied by the observation of the electromagnetic signals. These will provide information about the properties and behaviours of compact objects in this mass range.

*Michał BEJGER**

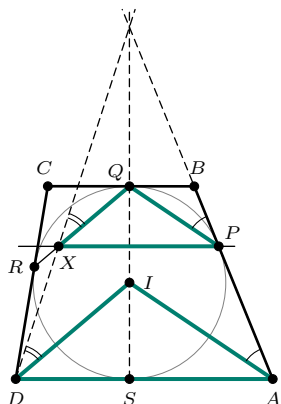
A. G. Abac et al., "Observation of Gravitational Waves from the Coalescence of a $2.5 - 4.5 M_\odot$ Compact Object and a Neutron Star", 2024, ApJL 970 L34.

*Nicolaus Copernicus Astronomical Center PAN, Istituto Nazionale di Fisica Nucleare (INFN), Sezione di Ferrara, Włochy

Solutions to the problems from page 9



Solutions to the problem M 1813.



Let I be the center of the inscribed circle in the considered trapezoid. Then

$$\sphericalangle IAP = \frac{1}{2} \sphericalangle DAB = \frac{1}{2}(180^\circ - \sphericalangle ABC) = \sphericalangle QPB,$$

hence $PQ \parallel AI$. Similarly, $DI \parallel QR$, so the triangles ADI and PXQ have corresponding sides parallel, and therefore they are homothetic. The center of this homothety is the point of intersection of the lines AB , QS , and DX .



Solutions to the problem M 1814.

Assume the opposite, i.e.,

$$a \leq 5b - \frac{4}{b^2}.$$

Then

$$5b - \frac{4}{b^2} + \frac{1}{a^2} \geq a + \frac{1}{a^2} \geq 5b - \frac{3}{b^2},$$

hence

$$\frac{1}{a^2} \geq \frac{1}{b^2},$$

so $a \leq b$. However, then

$$a + \frac{1}{a^2} \geq 5b - \frac{3}{b^2} \geq 5a - \frac{3}{a^2},$$

which means that

$$\frac{4}{a^2} \geq 4a,$$

so $a \leq 1$ – a contradiction.



Solutions to the problem M 1815.

We want to show that there exist positive integers a , b , and c such that

$$n + a^2 = (a + b)(a + c),$$

so it is enough for the number $n + a^2$ to be a product of two integers greater than a . Based on the assumptions of the problem, we can find such a prime number p and an integer $m > 0$ such that $n = p^2 m$. Consider four cases:

- 1) $m + 1 > p$. In this case, we can take $a = p$, since $n + a^2 = p^2 \cdot (m + 1)$ and both p^2 and $m + 1$ are greater than a .

- 2) $m + 1 < p$ and $m + 1$ is a composite number. Let $m + 1 = st$ for some integers $s, t > 1$. Again, we can take $a = p$, since $n + a^2 = ps \cdot pt$ and both ps and pt are greater than a .
- 3) $m + 1 < p$ and $m + 1$ is a prime number. Let $m + 1 = q$ and divide p by q with remainder: $p = \ell q + r$, where $r > 0$. Take $a = r$, then $n + a^2 = q \cdot (\ell^2 m q + 2\ell m r + r^2)$ and both factors are greater than r .
- 4) $m + 1 = p$. Then obviously $n = p^3 - p^2 > 20$, so we can assume $p \geq 4$. We have

$$n + 6^2 = (p + 3) \cdot (p^2 - 4p + 12),$$

where both factors on the right-hand side are greater than 6.

In each of these cases, we obtained the desired factorization, so the theorem has been proven.



Solutions to the problem F 1117.

After the rapid decrease in pressure, the water begins to evaporate throughout its entire volume. The resulting vapor absorbs heat from the liquid water, causing it to freeze (the water has a temperature of 0°C). The evaporation process is very fast, so the mass ratios of ice and vapor right after the pressure drop are determined only by the values of latent heat of vaporization and fusion. Let m_i denote the mass of ice produced. We have:

$$L_f \cdot m_i = L_v \cdot (m - m_i).$$

Solving for the mass of ice:

$$m_i = \frac{L_v m}{L_v + L_f}.$$

Numerically, $m_i \approx 8.71$ g. In equilibrium, which will be achieved as a result of further slow sublimation/resublimation processes, the mass of ice will also depend on the volume under the piston available for the water vapor.



Solutions to the problem F 1118.

In thermodynamic equilibrium, the average kinetic energies of helium and neon atoms are equal and proportional to the temperature in Kelvin. This means that their average velocities are inversely proportional to the square roots of their masses:

$$\frac{v_{\text{He}}}{v_{\text{Ne}}} = \sqrt{\frac{m_{\text{Ne}}}{m_{\text{He}}}} = \sqrt{5}.$$

If only one type of gas were present in the container, the time to empty the container of helium would be $\sqrt{5}$ times shorter than the time to empty it of neon. Since both gases can be treated as ideal gases, and the atoms do not interact with each other, the number of helium atoms escaping from the container per unit time will be $\sqrt{5}$ times greater than the number of neon atoms:

$$\frac{n_{\text{He}}}{n_{\text{Ne}}} = \sqrt{5}.$$

As the gas escapes, the composition of the beam will change because helium escapes faster than neon.



Rotations by Certain Special Angles

Bartłomiej BZDEGA

Adam Mickiewicz University in Poznań

In issue no. 74 (Δ_{25}^2), I wrote about central symmetry, which is the same as a 180° rotation around the center of symmetry. This time, the topic will be rotations by 90° and 60° . The general rule for using rotations in problem-solving is as follows: we rotate a part of the diagram in such a way that it fits in a different place.

For precision – all figures are given here with the order of vertices counterclockwise, and we also perform rotations in this direction.

Example 1. In square $ABCD$, points P and Q lie on sides BC and CD , respectively, with $|\angle PAQ| = 45^\circ$ (Fig. 1). Prove that $|BP| + |DQ| = |PQ|$.

Solution. Rotate triangle ABP around point A by 90° – we get triangle ADP' , which is congruent to ABP . The equalities $|\angle ADQ| = |\angle ADP'| = 90^\circ$ hold, so $|P'Q| = |DP'| + |DQ| = |BP| + |DQ|$. On the other hand, $|PQ| = |P'Q|$ because triangles APQ and AQP' are congruent (SSS).

A 60° rotation can be used to verify if a given triangle is equilateral. Triangle XYZ is equilateral if and only if one of the points X, Y, Z is the image of the other under a 60° rotation with respect to the third. An analogous rule can be formulated for the isosceles property of a right triangle, or even for any triangle.

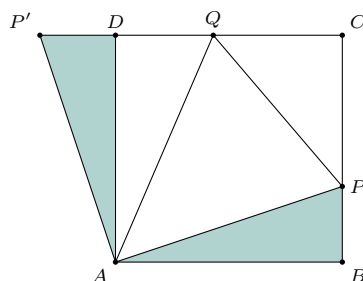


Fig. 1

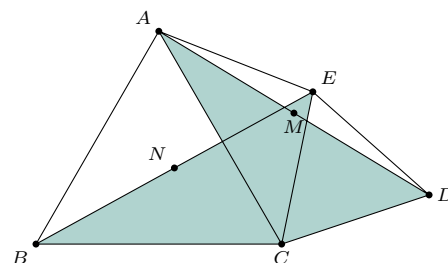


Fig. 2

Another general tip. If two congruent figures appear in a given geometric configuration, it's always worth checking what an isometry (for example, rotation) that transforms one into the other gives us.

Example 2. A convex pentagon $ABCDE$ is given, where triangles ABC and CDE are equilateral. Points M and N are the midpoints of diagonals AD and BE , respectively (Fig. 2). Prove that triangle CMN is equilateral.

Solution. Triangles ACD and BCE are congruent (SAS), the first is the image of the second under a 60° rotation around point C . The same rotation transforms point N into point M , so triangle CMN is equilateral.

Problems

- On the sides of triangle ABC , squares $BPQC$ and $CRSA$ are constructed. Points K and L are the midpoints of segments BR and AQ , respectively. Prove that triangle CKL is an isosceles right triangle.
- The common part of squares $ABCD$ and $APQR$ is point A . Point M is the midpoint of segment DP . Prove that $AM \perp BR$.
- A point P is located inside square $A_1A_2A_3A_4$. Line ℓ_i passes through point A_i and is perpendicular to $A_{i+1}P$ for $i = 1, 2, 3, 4$ (where we take $A_5 = A_1$). Prove that lines ℓ_1, ℓ_2, ℓ_3 , and ℓ_4 intersect at a single point.
- In triangle ABC , the median CM and the altitude CD are given. Through an arbitrary point P , lines perpendicular to AC, BC , and MC are drawn, intersecting line CD at points X, Y , and N , respectively. Prove that point N is the midpoint of segment XY .
- A convex quadrilateral $ABCD$ is given. The perpendicular bisectors of segments AB and CD intersect at point P , where $|\angle APB| = |\angle CPD| = 120^\circ$. Prove that the midpoints of segments AB, BC , and CD determine an equilateral triangle.
- Prove that all points X inside an equilateral triangle ABC that satisfy the equation $|AX|^2 + |BX|^2 = |CX|^2$ lie on a single circle.

Hints

- Compare with Example 2.
- Consider (congruent) parallelograms $ADVP$ and $BARX$. A 90° rotation around the center of square $ABCD$ transforms the first one into the second, so the image of line AV under this rotation is line BR .
- After a 90° rotation around the center of a given square, the line ℓ_i transforms into the line $A_{i+1}P$. Since after rotation all four lines have a common point P , this must also have been the case before the rotation.
- Mark the images of the points from the task as primed points under the 90° rotation. Triangle $X'Y'P$ is similar to triangle ABC , as it has corresponding sides parallel to those of triangle ABC . The line PN' contains the median of triangle $X'Y'P$ (why?), so point N' is the midpoint of segment $X'Y'$.
- Triangle APC after a 120° rotation transforms into triangle BPD , so $|AC| = |BD|$ and the acute angle between them is 60° .
- Let X be the point satisfying the conditions of the task. Rotate triangle ABX by 60° around point A – we obtain triangle ACX' . By the Pythagorean theorem, $|\angle CX'X| = 90^\circ$, so $|\angle AXB| = |\angle AX'C| = 150^\circ$.

Maths Beyond Limits



The 10th edition of the iconic international mathematical camp Maths Beyond Limits is approaching! MBL is a unique initiative bringing together young people passionate about mathematics from all around the world.

This year's camp will take place on **7-20.09.2025 in Rycerka Dolna, Poland**. We invite high school youth (ages 15-19) to apply through our website. Older maths enthusiasts are encouraged to apply to teach a class as a tutor.

Usual day at MBL:

mathematical classes

80-minute-long sessions devoted to some of the most beautiful concepts in mathematics from outside the high school's curriculum.

30-minute-long presentations on topics connected with mathematics given by participants.

camper talks

time academic unscheduled

During this time, tutors make themselves available for 'office hours' and groups often form to work together on problem sets.

various non-mathematical activities run by participants or organisers.

evening activities



www.mathsbeyondlimits.eu



mathsbeyondlimits@gmail.com



[mathsbeyondlimits](https://www.instagram.com/mathsbeyondlimits)



Maths Beyond Limits

In this issue you can find:

- materials from classes taught at MBL
- articles based on presentations of former camp participants